FTD-HT-23-241-70

FOREIGN TECHNOLOGY DIVISION

NUMERICAL STUDY OF IONIZATION INSTABILITY IN LOW-TEMPERATURE MAGNETIZED PLASMA

by

Ye. P. Velikhov, L. M. Degtyarev, and A. P. Favorskiy

EDITED TRANSLATION

NUMERICAL STUDY OF IONIZATION INSTABILITY IN LOW-TEMPERATURE MAGNETIZED PLASMA

By: Ye. P. Velikhov, L. M. Degtyarev, and A. P. Favorskiy

English pages: 76

Source: Chislennoye Issledovaniye Ionizatsionnoy Neustoychivosti v Nizkotemperaturnoy Zamagnichennoy Plazme, Academy of Sciences of the USSR, Institute of Applied Mathematics, 1969, 112 pages.

Translated by: J. Miller/TDBRS-3

TABLE OF CONTENTS

Annotation

In this work we examine the statement and numerical solution of the problem of the development of ionization instability in a low-temperature magnetized plasma. Basic attention is devoted to the dynamics of the development of instability and a qualitative analysis of the phenomenon. We show the effectiveness of the physical model used as the basis of the examination. As a result of the numerical calculations, we refine the association between the average parameters of the plasma at process stages close to turbulence.

CHAPTER 1

INTRODUCTION

Recently much attention has been paid to the study of the phenomenon of ionization instability in a nonuniformly ionized low-temperature plasma in a magnetic field.

First, it appeared that this phenomenon is of practical significance for MHD generators and accelerators using atomic gases. It appears simultaneously with the separation of electron temperature from the temperature of heavy particles. In a sufficiently strong magnetic field the ionization instability determines the effective conductivity of the plasma.

Second, ionization instability apparently leads to one of the few forms of turbulence which is most accessible to theoretical and experimental investigation. The relatively simple structure of the energy equation makes it possible, in a number of cases, to construct simplified mathematical models of the phenomenon; we are able to examine an already developed process, and not merely its initial stage. The results of the theory describe qualitatively, to a certain degree, the basic regularities known from experiment. In particular, in a number of cases the increase in effective resistance with magnetic field is predicted theoretically and confirmed experimentally. From dimensional concepts it is to be expected that in a turbulent plasma with magnetized electrons the resistance should be defined by the relationship

$$\rho = \frac{cB}{en_e} \qquad (1)$$

where B is the magnetic field, c is the speed of light, e is the electron charge, and n_e is the electron concentration. This formula, as can be easily seen, corresponds to the familiar Bohm formula for turbulent diffusion of plasma.

An essential understanding of the phenomenon was also achieved in experimental study. This was aided by the short duration of the characteristic time of development of the instability, which made it possible to isolate it in "pure" form, i.e., to avoid the influence of other instabilities (ion sound, etc.). This is an additional reason for interest in ionization instability, whose study is thus important both from an applied as well as a general physical point of view. Up to the present time a great many experimental and theoretical works have been devoted to this phenomenon. Let us give a brief summary of certain of these.

Attention was first paid to the possibility of the origination of ionization instability in [1] and [2], and also independently in [3].

Reference [2] gave a one-dimensional nonlinear theory.

It was shown that the development of one-dimensional fluctuations leads to a state with the effective resistance

$$\rho \approx \frac{cB}{2en_e}. \qquad (2)$$

The quasi-linear method used in this work was not valid far from the stability boundary. The results of the work were refined by Zampalioni [17] and Solbes [16]; however, the final result of [2] was correct. In [3] Ohm's law is proposed and compared with experiment, taking into account fluctuations in electron and gas temperature. The possibility is indicated of "complete" instability of a weakly-ionized plasma. The work is limited to the frameworks of the linear theory.

One of the first experiments is described in [4]. It is shown that the effective conductivity across the magnetic field decreases as $\sim\frac{1}{B}$; the assumption is made that the drop in conductivity is explained by ionization instability.

In [5], using an electron-optical converter, there was obtained an instantaneous photograph of the distribution of electron density (and current) in a plane perpendicular to the magnetic field. There was detected the existence of well-developed striations at an angle of ~30°-40° to the current. Qualitatively, the result coincided with theory, although a complete explanation of the structure was obtained only upon numerical solution of the nonlinear boundary problem [23-25]. Further, a detailed study was made of the condition of origination of instability, the influence of the transport of resonance radiation, the influence of current along the magnetic field, and systems of conductors creating "rigid equipotentials" and stabilizing the instability. The basic conclusion of the work was that suppression of the ionization instability is almost as unsuitable, energywise, as reconciliation with its existence. Calculation was made of a model of nonlinear development of ionization instability with time, which led to relationship (2) for effective resistance of the plasma, and a model of developed turbulence was proposed.

Experimentally, [6] is a development of [5]. It gives the results of a photographic study of instability in a discharge. The structure of the nonuniformities and the influence of the degree of ionization are studied.

Experimental works [7-10] investigate the development of ionization instability in a disk channel. The use of a disk channel makes it possible to avoid the influence of electrodes, while various types of pre-ionizers make it possible to study the dependence of the development of ionization instability on the initial conditions. It is shown that independently of conditions at the inlet ionization instability occurs and there is saturation of the effective Hall parameter. In experiments [10] with thermal ionization in a frozen flow with complete ionization of the admixture, ionization instability

does not develop. In experiments [9] it was detected that with total ionization of its cesium admixture in helium, saturation of the Hall parameter appears with relatively low concentration fluctuations. In this series of experiments the nature of the saturation of the Hall relationship with total ionization remains unexplained. In work [11] there were conducted measurements of the effective parameter in an equilibrium plasma with a CO_2 additive. It was shown that saturation of the Hall parameter is nonexistent up to values $\Omega \sim 5$. Thus, phenomena in the disk channel actually are determined, apparently, by instability.

The flow of inert gases with alkali metal additives in a Faraday-type MHD channel was studied in [12-13]. It was shown that at high current densities ionization instability has a strong influence on the effective conductivity and the Hall parameter.

Work [14] investigated the development of ionization instability in a discharge across a flow and a magnetic field. Study of the geometry of the fluctuations showed that with sufficiently large current densities ionization instability actually developed.

Work [15] theoretically investigated the development, with time, of a nonlinear one-dimensional wave. Further calculations are given in [16].

Theoretical survey [17] discusses in detail questions of the ionization equilibrium and energy balance in a plasma with detachment of the electron temperature and stability of a nonequilibrium plasma.

Work [18] calculates the effective conductivity of plasma with two-dimensional nonuniformity. It is shown that even weak isotropy of the fluctuations leads to a law of linear increase in effective resistance with the magnetic field for a given amplitude and spectrum of the fluctuation.

The development of ionization instability in a system with given boundary conditions causes basic difficulties even in linear statement

of the problem because of the absence of natural modes. The problem of the evolution of an initial perturbation with ideal segmentation of the electrodes has been solved in [19]. It was shown that initial perturbations increase nonexponentially, although the criterion of stability is practically the same as in an unbounded region.

In [20-21], following works [2] and [5], there is calculated the quasi-linear development of ionization instability near the threshold. It is shown that asymptotically the following laws are satisfied:

$$\sigma_{eff} \sim \Omega_{cr}/\Omega \qquad \Omega_{cr} \sim \sigma_{eff}.$$

Later these relationships were used as the basis of one-dimensional calculation of MHD generators. The first work of this type was [22].

Works [23-25] solved numerically the problem of the development of ionization instability in a strongly magnetized plasma. It was found that the initial perturbation develops in striations which then are destroyed and the picture becomes close to turbulent. Finally, work [26] is analogous to [23-25], but here there is examined only the initial stage of striation formation.

On the basis of this brief survey we can conclude that analytical examination of ionization instability is extremely difficult. Nonlinear analysis has been performed only in one-dimensional approximation. At the same time the influence of boundary effects, as experiments showed, can in certain cases have decisive influence even on the qualitative nature of the process. However, the two-dimensional problem is difficult for analytical examination even in linear approximation.

In such cases, an effective method of investigation can be calculation experiment, which helps to overcome the mathematical difficulties in the theory and fulfills the physical experiment which gives a limited amount of information due to measurement difficulty.

This present work is a development of [23-25] and is devoted to a discussion of a number of numerical experiments on the development of ionization instability in various models of nonequilibrium plasma.

CHAPTER 2

PHYSICAL ASSUMPTIONS AND EQUATIONS

We examine a quasi-neutral, dense, low-temperature plasma. We will consider the plasma to be atomic, i.e., we will exclude from our examination the interaction of electrons with molecular compounds. Then the characteristic time for energy exchange between the electrons is considerably less than with heavy particles because of the considerable difference in masses (ions and neutral atoms). Because of this, the energy connection of the electrons with the heavy component is weak, and the electron gas of free electrons and electrons occupying discrete energy levels of the atoms forms an almost closed equilibrium system.

This indicates that there occurs Maxwellian distribution of free electrons and Boltzmann distribution of electrons which are in the excited levels of atoms, characterized by electron temperature T_e. Collisions with heavy particles, as has already been noted, only weakly influence the deviation from thermodynamic equilibrium of the electrons, but define the value of electron temperature T_e.

The basic reason for disruption of equilibrium in a cold plasma is the radiation of the electrons of excited atoms in a discrete spectrum. Here a correct theoretical description of the radiation transport process is given only by the kinetic approach. The fact of the matter is that, together with photons in the center of the line, having small free path lengths because of resonance absorption, an essential role is played by photons on the "wings of the line," whose

free path length is commensurate with the dimension of the plasma itself. Radiation leads to three effects: deviation from Maxwellian distribution of the free electrons, deviation from Boltzmann distribution of electrons on excited levels of the atoms, and cooling of the plasma as a whole. Estimates given in [17] together with the results of experimental works show that in a sufficiently dense plasma ($n_e > n_{cr} \sim 10^{13}$ 1/cm^3; n_e is the concentration of free electrons) at temperatures $T_e \sim 0.3$ eV we can disregard the deviation of the electron gas from equilibrium because of radiation. But in dense atomic plasma as well the contribution of radiation to the electron energy balance is completely commensurate with other transport processes.

Let us discuss further a simple model of an atomic two-temperature plasma. The light component consists of an equilibrium electron gas with temperature T_e, concentration of free electrons n_e, and electrons in the excited level of the atoms. The heavy component consists of ions and neutral atoms with concentration $n_i + n_a$ and temperature T. To be specific, we have in mind an inert gas (e.g., Ar) with a slight addition of a lightly ionized admixture (e.g., Cs). In this case the concentration of electrons and ions n_e coincides with the number of ionized atoms of the admixture per unit volume and does not exceed the concentration of the admixture n_s (we consider only single ionization).

With application of an electrical and magnetic field, there occurs in the plasma an electric current whose density $\vec{j}$ is associated with the strength of the electrical $\vec{E}$ and magnetic $\vec{H}$ fields by the generalized Ohm's law [31-32]. In our case we can disregard inertia of the electrons and "slip" of the ions relative to the neutral atoms. Conservation of momentum of the electrons for a Lorentz gas under these assumptions gives Ohm's law in the form

$$\vec{j} + \vec{j} \times \vec{\Omega} = \sigma \vec{E}' - \frac{e}{m\nu} \nabla p_e, \quad \vec{\Omega} = \frac{e\vec{H}}{m_e c} \tag{2.1}$$

where σ is the conductivity, defined by the expression

$$\sigma = \frac{e^2 n_e}{m_e c \nu} \tag{2.2}$$

p_e is the gas pressure of the free electrons; $\vec{E}'$ is the electrical field in a system of coordinates moving with the mean-mass flow rate.

Here and henceforth we will use the standard designations:

e is the electron charge,
m_e is the electron mass,
c is the speed of light,
M is the mass of an atom,
I is the ionization potential,
ν_i is the collision frequency of an electron with ions,
ν_a is the collision frequency of an electron with atoms,
k is the Boltzmann constant.

Now let us write the energy balance of an electron gas per unit volume per unit time. According to the first law of thermodynamics it can be represented as follows:

$$\frac{d}{dt}[n_e(I + \tfrac{3}{2}kT_e)] = Q - Q_s - p_e \times \\ \times \operatorname{div} \vec{v} - n_e(I + \tfrac{3}{2}kT_e) \operatorname{div} \vec{v} - \operatorname{div} \vec{q}. \tag{2.3}$$

Let us examine, in sequence, all components of the right side of the equation. The first term defines the magnitude of the contribution of Joule heating per unit volume:

$$Q = \frac{j^2}{\sigma}. \tag{2.4}$$

The second term characterizes the output of electron energy during collisions with heavy particles:

$$Q_s = m_e n_e \tfrac{3}{2}k(T_e - T)\sum_\alpha \delta_\alpha \frac{\nu_\alpha}{M_\alpha} \tag{2.5}$$

where δ_α is a constant which is defined by mechanisms of collision of an electron with an α-type heavy component.

The work of electron pressure is described by the third term in equation (2.3). The other components, in sequence, show the change in energy of electrons due to transport processes: convective radiation and heat flux $\vec{q}$. The connection between concentration n_e and temperature T_e of the electrons is given by the equation of ionization kinetics. Let us assume that there occurs only thermal ionization by electron impact:

$$a + e = i + e + e \tag{2.6}$$

while the inverse process is recombination with triple collision:

$$i + e + e = a + e. \tag{2.7}$$

The equation of the kinetics for such a reaction has the form

$$\frac{dn_e}{dt} = \alpha \cdot n_e \cdot n_a - \beta n_i n_e^2. \tag{2.8}$$

The constants of ionization α and recombination β rates are connected by the principle of detailed equilibrium:

$$\frac{\alpha}{\beta} = K(T_e). \tag{2.9}$$

The equilibrium constant $K(T_e)$ in an equilibrium electron gas is defined by the Saha formula:

$$K(T_e) = \frac{n_e n_i}{n_a} = \frac{2g_i}{g_a}\left(\frac{2\pi m_e kT_e}{h^2}\right)^{3/2} e^{-\frac{I}{kT_e}} \tag{2.10}$$

where g_i and g_a are the static weights of an ion and a neutral atom, respectively.

The description of this model of the plasma is closed by the Maxwell equations. As usual, let us disregard the displacement currents $\frac{1}{c}\frac{\partial \vec{E}}{\partial t}$ as compared with conductivity currents $\frac{4\pi}{c} \cdot \vec{j}$. Let us also assume that the induced magnetic field $\vec{h} \sim \frac{4\pi}{c} j_0 L_0$ (j_0 is the average value of electric current density, L_0 is the characteristic dimension of the plasma) is considerably less than the applied field $\vec{H}$. In this case the equations of electrodynamics express the law of conservation of electric charge:

$$\operatorname{div} \vec{j} = 0 \qquad (2.11)$$

and potential of the electric field

$$\operatorname{curl} \vec{E} = 0. \qquad (2.12)$$

Let us assume that the external magnetic field in which the plasma is located has only one component. Then the direction along the magnetic field $\vec{H}$ is isolated, since along it the mobility of the electrons is considerably higher than in any other direction perpendicular to $\vec{H}$. Therefore the problem can be considered to be two-dimensional, and it can be examined in the plane normal to the magnetic field. Without restricting generality let us assume that the plasma occupies a rectangular volume ABCD (Fig. 1) whose walls are an ideal dielectric excluding electrodes ab and cd, which are either ideally sectioned or compact and ideally conducting. On the dielectric portion, obviously, $j_n = 0$. On an ideally sectioned electrode we are given the electric current density j_n, while on the ideally conducting electrode the condition $E_\tau = 0$ should be satisfied and we are given the total current J flowing between the electrodes.

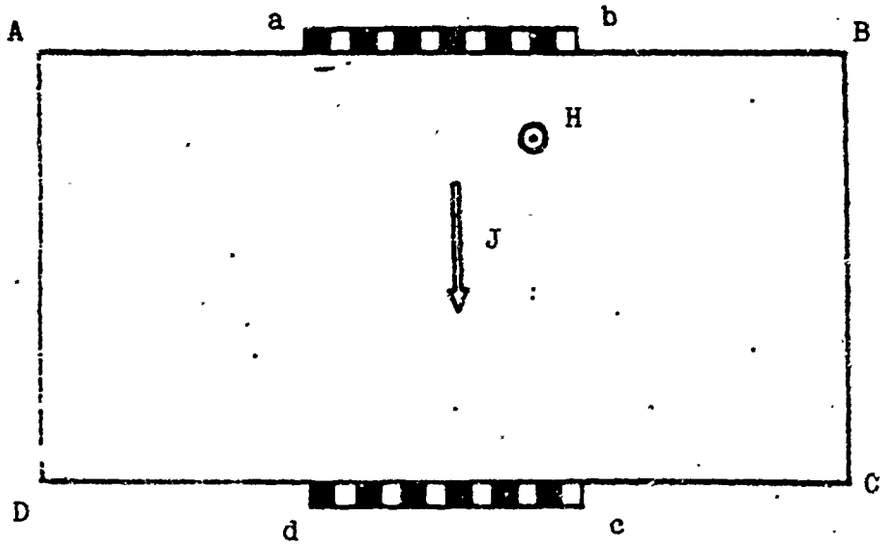

Fig. 1.

This statement, borrowed from an experiment in which ideally sectioned electrodes completely occupy the horizontal portions of the

boundary, make it possible to trace the development of ionization instability caused by a perturbation introduced into a stationary field of electric currents [23-25]. When on the horizontal boundary there are portions of an ideal dielectric, the problem simulates the development of instability in an MHD channel. Finally, the presence of a compact ideally conducting electrode makes it possible to consider its influence on the turbulent plasma.

CHAPTER 3

DIMENSIONAL ANALYSIS

Let us formulate more specifically the statement of the problem which will be examined in what follows. Let us assume that in a quiet plasma there is no radiant heat transport or heat flow. We will also consider that the electron temperature considerably exceeds the gas temperature $T_e \gg T_i$, but at the same time the average thermal energy of the electron is low in comparison with the ionization potential $I \gg \frac{3}{2}kT_e$. The collision frequency of an electron with the neutral component is defined by the expression

$$\nu_a = [\sigma_g n_g + \sigma_s(n_s - n_i)]\langle|v_e|\rangle \tag{3.1}$$

while the frequency of electron collisions with ions

$$\nu_i = \sigma_i\langle|v_e|\rangle n_i. \tag{3.2}$$

Here σ_g, σ_s, and σ_i are the collision cross sections of an electron with atoms of an inert gas, the admixture, and ions, respectively; $\langle|v_e|\rangle$ is the average value of the thermal velocity of an electron; n_g, $n_s - n_i$, and n_i are, respectively, the concentrations of atoms of an inert gas, admixture, and ions. The total frequency of collisions undergone by an electron

$$\nu = \nu_i + \nu_a. \tag{3.3}$$

We will assume, in addition, the following dependence of cross sections σ_i, σ_s, and σ_g and the average thermal velocity $\langle|v_e|\rangle$ on temperature T_e:

$$\sigma_i = \sigma_1 T_e^{-2},\ \sigma_s = \sigma_2,\ \sigma_g = \sigma_3 \tag{3.4}$$

$$\langle |v_e| \rangle = \left(\frac{3kT_e}{m_e}\right)^{1/2} \tag{3.5}$$

where σ_1, σ_2, and σ_3 are constants. Then for the total number of collisions we get the expression

$$\nu = A_1' n_e T_e^{-3/2} + A_2' T_e^{1/2}(n_s - n_e) + A_3' T_e^{1/2} n_g$$
$$A_1' = \sigma_1\left(\frac{3k}{m_e}\right)^{1/2},\ A_2' = \sigma_2\left(\frac{3k}{m_e}\right)^{1/2},\ A_3' = \sigma_3\left(\frac{3k}{m_e}\right)^{1/2}. \tag{3.6}$$

Under these additional assumptions the initial system of equations obtained in the previous section assumes the form:

$$\vec{j} + \vec{j} \times \vec{\Omega} = \sigma \vec{E}' - \frac{e}{m_e \nu} \nabla p_e,\ \sigma = \frac{e^2 n_e}{m_e \nu},\ \vec{\Omega} = \frac{e\vec{H}}{m_e c} \tag{3.7}$$

$$I\frac{dn_e}{dt} = \frac{j^2}{\sigma} - \delta n_e \nu \frac{m_e}{M} kT_e,\ \nu = A_1' m_e T_e^{-3/2} +$$
$$+ A_2' T_e^{1/2}(n_s - n_e) + A_3' T_e^{1/2} n_g \tag{3.8}$$

$$\frac{dn_e}{dt} = \alpha n_a n_e - \beta n_i n_e^2,\ \frac{\alpha}{\beta} = \frac{2g_i}{g_a}\left(\frac{2\pi m_e kT_e}{h}\right)^{3/2} e^{-\frac{I}{kT_e}} \tag{3.9}$$

$$\operatorname{div} \vec{j} = 0 \tag{3.10}$$

$$\operatorname{curl} \vec{E} = 0. \tag{3.11}$$

Let us reduce (3.7)-(3.11) to dimensionless form. As the characteristic scales of the problem we select the initial value of electron concentration n_0 at a certain point in space, temperature T_0, and electrical conductivity σ_0. The scales for measuring the other magnitudes are expressed from equations (3.7)-(3.9). From expressions (3.7) for electrical conductivity we have the scale of measurement of the collision frequency:

$$\nu_0 = \frac{e^2 n_0}{\sigma_0 m_e}. \tag{3.12}$$

The dimensionless expression of equation (3.6) assumes the form

$$\nu = A_1 n_e T_e^{-3/2} + A_2 T_e^{1/2}(n_s - n_e) + A_3 T_e^{1/2} n_g \tag{3.13}$$

Here n_s is the reciprocal of the degree of ionization of the admixture at the initial moment of time. The values of the dimensionless constants A_1, A_2, and A_3 are defined from the condition $\nu = 1$ at the initial moment of time, i.e.,

$$A_1 + (1 - n_s)A_2 + n_g A_3 = 1 \tag{3.14}$$

and the equalities

$$\frac{A_1}{A_2} = \frac{\sigma_1}{\sigma_2}, \quad \frac{A_2}{A_3} = \frac{\sigma_2}{\sigma_3}. \tag{3.14'}$$

From (3.14) and (3.14') for A_1, A_2, and A_3 we get the values

$$A_1 = \frac{\sigma_1}{\sigma_1 + (n_s - 1)\sigma_2 + n_g\sigma_3}, \quad A_2 = \frac{\sigma_2}{\sigma_1 + (n_s - 1)\sigma_2 + n_g\sigma_3},$$

$$A_3 = \frac{\sigma_3}{\sigma_1 + (n_s - 1)\sigma_2 + n_g\sigma_3}. \tag{3.15}$$

From energy equation (3.8) it follows that the characteristic time of the problem

$$t_0 = \frac{I}{\kappa k T_e \nu_0}, \quad \kappa = \delta\frac{m_e}{M} \tag{3.16}$$

whence we obtain the scale of the measurement for electric current density

$$j_0 = \left(\frac{I\sigma_0 n_0}{t_0}\right)^{1/2}. \tag{3.17}$$

From Ohm's law (3.7) the scales for electrical field E_0 and the mean-mass rate V_0 have the values

$$E_0 = j_0/\sigma_0, \quad V_0 = c\frac{E_0}{H_0} \tag{3.18}$$

while the measurement scale for the magnetic field

$$H_0 = \frac{mc\nu_0}{e} \tag{3.19}$$

is such that the dimensionless value of the magnetic field is equal to the Hall parameter at the initial moment of time. Let us estimate the contribution of electron pressure $p_e = kn_eT_e$ to Ohm's law as compared with the other terms. Let us examine the relationship

$$\gamma = \frac{ep_{e0}}{m_e\nu_0L_0j_0}. \tag{3.20}$$

Here p_{e0} is the characteristic value of electron pressure. Using (3.12) and (3.18) we get

$$\gamma = \frac{kT_{e0}}{eE_0L_0}. \tag{3.21}$$

For MHD converters and most experiments the following condition is valid:

$$\frac{3}{2}kT_e \ll eEL$$

i.e., the mean thermal energy of an electrode is low as compared with the characteristic difference in potentials. From this it follows that the electron pressure gradient in Ohm's law can be disregarded. Let us turn to the equation of ionization kinetics (3.9). With low degrees of ionization we see from this equation that the characteristic time of a change in concentration of electrons is expressed by the value

$$\tau = \frac{1}{n_e\alpha_0} \tag{3.22}$$

where α_0 is the scale of measurement of the ionization rate, which is expressed by the formula

$$\alpha = \frac{\sigma_\alpha}{n_e}\int\limits_{|v| > v_0} vf(v)dv \tag{3.23}$$

α_a is the interaction cross section of an electron with an atom, v_0 is the minimum velocity of the electron of ionizing atoms of the admixture, and f(v) is the distribution function for free electrons with respect to velocities. Considering that Maxwellian velocity distribution is valid for electrons, for α we get the expression

$$\alpha = \sigma_a \left(\frac{kT_e}{2\pi m_e}\right)^{1/2} e^{-I/kT_e} \tag{3.24}$$

respectively for

$$\alpha_0 = \sigma_a \left(\frac{kT_{e0}}{2\pi m_e}\right)^{1/2} e^{-\frac{I}{kT_{e0}}}. \tag{3.25}$$

Comparing the characteristic times t_0 and τ, we find, assuming that $\nu_0 \simeq n_0\alpha_0$,

$$\frac{\tau}{t_0} = \frac{\kappa k T_{e0}\nu_0}{n_a\alpha_0 I} \sim \frac{s \cdot m_e T_{e0} k}{M \cdot I}. \tag{3.26}$$

Henceforth we will assume that the plasma has parameters for which $\tau/t_0 \ll 1$, i.e., the thermal ionization is quasi-equilibrium and, consequently, instead of equation (3.9) we can use the principle of detailed equilibrium:

$$\frac{n_i n_e}{n_a} = \frac{n_e^2}{n_s - n_e} = \frac{2g_i}{g_a}\left(\frac{2\pi m_e kT_e}{h^2}\right)^{3/2} e^{-\frac{I}{kT_e}}. \tag{3.27}$$

In dimensionless form (3.27) assumes the form

$$\frac{n_e^2}{n_s - n_e} = n_* T^{3/2} e^{-\frac{k_0}{T_e}} \tag{3.28}$$

where

$$k_0 = I/kT_0 \tag{3.29}$$

and

$$\frac{\partial \psi}{\partial y} = \Omega \frac{\partial \psi}{\partial x}. \tag{4.3}$$

Thus, in the general case, for equation (4.2) on a section of the boundary we are given the first boundary-value problem

$$\psi|\Gamma = \nu(s) \tag{4.4}$$

where s is a length of arc along boundary Γ, while in the remaining section (it may be absent) we have the condition (4.3), i.e., there occurs a mixed boundary-value problem.

To solve the equation

$$\frac{dn_e}{dt} = \frac{j^2}{\sigma} - n_e \nu T_e$$
$$\nu = A_1 n_e T_e^{-3/2} + A_2 (n_s - n_e) T_e^{1/2} + A_3 n_g T_e^{1/2} \tag{4.5}$$

we are required to give only the initial condition

$$n|_{t=0} = n_0(x, y). \tag{4.6}$$

The form of the function $n_0(x, y)$ will be selected below when examining specific examples. As linear analysis shows, problem (4.2)-(4.6) is correct, but unstable. For the unbounded linear problem the perturbations increase exponentially with time, while for the linear boundary-value problem [19] the increase in perturbation occurs nonexponentially. Let us note further that since the differential operator of equation (4.2) is not self-conjugate, in it actual eigenfunctions are absent.

Nonlinear system (4.2)-(4.6) was integrated numerically. In this regard let us note that there are no diffusion terms in differential equation (4.5). However during numerical solution of the problem there appears an averaging scale λ equal to the step of the difference network h. When solving the problem, taking into account diffusion processes (thermal conductivity, radiation, etc.), the diffusion length of these processes is the characteristic dimension of averaging. From this standpoint the step of the difference scheme can be treated as the diffusion length of certain physical properties. Thus the

$$n_* = \frac{1}{n_0}\frac{2g_i}{2g_a}\left(\frac{2\pi m_e kT_{e0}}{h^2}\right)^{3/2}. \qquad (3.30)$$

Bearing in mind that the scales n_e and T_e are their initial values, satisfying (3.27), the magnitude can be found from the equality

$$n_* = e^{k_0}/(n_s - 1). \qquad (3.31)$$

Finally, let us formulate the equations which describe the process in dimensionless variables:

$$\frac{dn_e}{dt} = \frac{j^2}{\sigma} - n_e \cdot \nu \cdot T_e \qquad (3.32)$$

$$\nu = A_1 n_e T_e^{-3/2} + A_2(n_s - n_e)T_e^{1/2} + A_3 n_g T_e^{1/2} \qquad (3.33)$$

$$\frac{n_e}{n_s - n_e} = n_* T^{3/2} e^{-k_0/T_e} \qquad (3.34)$$

$$\vec{j} + \vec{j} \times \vec{\Omega} = \sigma(\vec{E} + \vec{v} \times \vec{H}),\ \vec{\Omega} = \vec{H}/\nu,\ \sigma = n/\nu \qquad (3.35)$$

$$\operatorname{div} \vec{j} = 0 \qquad (3.36)$$

$$\operatorname{curl} \vec{E} = 0. \qquad (3.37)$$

Let us examine, as an example, values of the dimensionless parameters for a plasma of cesium vapors. Let us assume that at the initial moment t = 0 the electron temperature T_e = 2900°K and the degree of ionization α = 1/3 (the electron concentration $n_e = 6.9 \cdot 10^{16}$ $1/cm^3$). Then we find that k_0 = 10 and n_s = 3. Knowing the conductivity of such a plasma at the initial moment of time σ_0 we can find the values of the remaining dimensional parameters.

CHAPTER 4

MATHEMATICAL STATEMENT OF THE PROBLEM

The distribution of electric fields E_x, E_y and currents j_x, j_y is conveniently described using the vector-potential of the electrical current $\vec{\psi}$. In the examined case of a two-dimensional problem we can consider that only its z-component is different from zero; this we designate by ψ. By definition of the vector-potential:

$$j_x = \frac{\partial \psi}{\partial y}, \quad j_y = -\frac{\partial \psi}{\partial x}. \tag{4.1}$$

Thus, knowing function ψ, we can seek the distribution of currents j_x, j_y. Excluding j_x, j_y and E_x, E_y from equations (3.35)-(3.37), using (4.1) we get an equation for ψ:

$$\frac{\partial}{\partial x}\left(\frac{1}{\sigma}\frac{\partial \psi}{\partial x}\right) + \frac{\partial}{\partial y}\left(\frac{1}{\sigma}\frac{\partial \psi}{\partial y}\right) + \frac{\partial}{\partial x}\left(\frac{\Omega}{\sigma}\frac{\partial \psi}{\partial y}\right) - \frac{\partial}{\partial y}\left(\frac{\Omega}{\sigma}\frac{\partial \psi}{\partial x}\right) = 0, \tag{4.2}$$

$$\Omega = 1/\nu, \quad \sigma = n/\nu.$$

As has already been mentioned, we will examine rectangular region ABCD (Fig. 1), whose boundary is an ideal dielectric, excluding electrodes ab and cd. On the dielectric sections aACc and bBDd, ψ = const. Considering the arbitrariness in defining ψ, let us set $\psi = 0$ on aACc, and $\psi = \psi_1 = J_0$ on bBDd, where J_0 is the current passing between the electrodes. Electrodes ab and cd will be considered either ideally sectioned with constant current density $j = J_a/L_{ab}$, or ideally conducted. In the first case, on sections ab and cd we are given function ψ as linearly increasing from 0 to ψ_1. In the second case $E = E_x = 0$ on sections ab and cd leads to the need for giving a condition with the "directional derivative"

$$\frac{\partial \psi}{\partial y} = \Omega \frac{\partial \psi}{\partial x}. \tag{4.3}$$

Thus, in the general case, for equation (4.2) on a section of the boundary we are given the first boundary-value problem

$$\psi|\Gamma = \nu(s) \tag{4.4}$$

where s is a length of arc along boundary Γ, while in the remaining section (it may be absent) we have the condition (4.3), i.e., there occurs a mixed boundary-value problem.

To solve the equation

$$\frac{dn_e}{dt} = \frac{j^2}{\sigma} - n_e \nu T_e$$
$$\nu = A_1 n_e T_e^{-3/2} + A_2 (n_s - n_e) T_e^{1/2} + A_3 n_g T_e^{1/2} \tag{4.5}$$

we are required to give only the initial condition

$$n|_{t=0} = n_0(x, y). \tag{4.6}$$

The form of the function $n_0(x, y)$ will be selected below when examining specific examples. As linear analysis shows, problem (4.2)-(4.6) is correct, but unstable. For the unbounded linear problem the perturbations increase exponentially with time, while for the linear boundary-value problem [19] the increase in perturbation occurs nonexponentially. Let us note further that since the differential operator of equation (4.2) is not self-conjugate, in it actual eigenfunctions are absent.

Nonlinear system (4.2)-(4.6) was integrated numerically. In this regard let us note that there are no diffusion terms in differential equation (4.5). However during numerical solution of the problem there appears an averaging scale λ equal to the step of the difference network h. When solving the problem, taking into account diffusion processes (thermal conductivity, radiation, etc.), the diffusion length of these processes is the characteristic dimension of averaging. From this standpoint the step of the difference scheme can be treated as the diffusion length of certain physical properties. Thus the

change in step in the difference net leads to a change in the characteristic scale of the problem. Nonlinear system (4.2)-(4.6) was numerically integrated as follows. First we found the solution of the steady-state equation (4.2) with coefficients calculated from the values of electron concentration n_e from the previous time level. Then, according to the difference analog, equations (4.5) were recalculated for values of n_e at the new moment of time. The boundary value problem for equation (4.2) has a number of specific features which should be taken into account when solving it numerically. The basic ones of these are as follows:

1. The values n, ν, and σ can be highly variable in space.

2. The differential operator is not self-conjugate.

3. On an ideally conducting electrode there is a condition with a "directional derivative."

4. The value σ on a certain previously unknown section can vanish.

The calculating algorithm was developed on the basis of [27-28]. A detailed exposition of the methodological questions is given in [29].

CHAPTER 5

RESULTS OF NUMERICAL CALCULATIONS. DISCUSSION

1. Let us begin the examination with the simplest statement in which, nonetheless, the characteristic features of the studied phenomenon are expounded. Let us assume that in rectangular region ABCD (Fig. 1) there is a plasma with constant concentration of free electrons $n_e = 1$.

The external magnetic field is also constant throughout the region. In the plasma, between the ideally sectioned electrodes ab = AB = 1, and cd = CD = 1, there flows a constant and uniform electric current:

$$j_x = 0, \quad j_y = -1.$$

Walls AD = 2 and BC = 2 are made of an ideal dielectric on which $j_x = 0$. The assumed values of the electric current density and electron concentration are, formally, the solution of steady-state equations (4.1-4.6) which, however, as will be seen from what follows, is unstable.

Let us assume that at moment t = 0 there is a perturbation of the three-dimensional distribution of electron concentration. We will be interested in the further time behavior of concentration n_e, of the vector field of the electric current density j_x, j_y, and also the integral and average characteristics. These latter play a very substantial role in the study of the process. In this present work we introduce into examination

$$\langle n\rangle = \frac{1}{s_{ABCD}} \iint_{ABCD} n_e dxdy$$

$$\langle \tau\rangle = \frac{1}{s_{ABCD}} \iint_{ABCD} \frac{1}{\nu} dxdy$$

$$\langle E_x\rangle = \frac{1}{s_{abcd}} \iint_{ABCD} E_x dxdy$$

$$\langle E_y\rangle = \frac{1}{s_{abcd}} \iint_{ABCD} E_y dxdy.$$

When constructing the average $\langle E_x\rangle$ and $\langle E_y\rangle$ it was considered that the region in which the electric field is effectively present comprises part of region ABCD. To be specific, we will arbitrarily consider that this is the interelectrode area s_{abcd}. In addition we will trace the minimum n_{min} and maximum n_{max} concentrations of free electrons in region ABCD. Of great interest are the effective conductivity of the plasma

$$\sigma_{eff} = \langle j\rangle/\langle E_j\rangle$$

and the effective Hall ratio

$$\beta_{eff} = \langle E_\perp\rangle/\langle E_j\rangle.$$

In the examined statement $\langle j\rangle = \langle j_y\rangle$ and, consequently,

$$\sigma_{eff} = \langle j_y\rangle/\langle E_y\rangle$$

$$\beta_{eff} = \langle E_x\rangle/\langle E_y\rangle.$$

In all the calculations to be described in Sections 1.1 and 1.2 the number of cells was taken as N = 200, while the averaging scale λ (the step of the difference network) was assumed as h = 0.1. A perturbation was performed on the value Δn_e in a rectangle consisting of several cells. The shape of the rectangle, its position, and also the amplitude and sign of perturbation were varied.

1.1. It is natural to begin with a Coulomb model of a plasma, additionally assuming that $T_e = 1$; then $\nu = n_e$, $\sigma = 1$. As calculations showed, the process of the development of ionization instability can be arbitrarily divided into two stages. In the first stage, in a

certain characteristic time $t = t^* \sim 1$, ionization instability leads to the occurrence of regular formations in which $n_e > 1$, separated by regions of lesser concentration $n_e < 1$. In shape and location these formations can be compared with striations observed in the experiment. Figure 2 shows lines of the level $n_e = 1$ at time $t = 1.5$ for the case $\Omega = 10$. A perturbation with amplitude 0.2 at $t = 0$ occupied eight cells in the central part of the region shown in Fig. 2. The regions with $n_e > 1$ are cross-hatched. The induced electric currents are of a vortex nature and flow along closed lines (Fig. 2). Combining with the external current, they cause the resulting current to flow primarily along the striations within which the intensive Joule heating is accompanied by ionization. Attenuations of the resulting current and Joule heating, however, in the "wells" leads to a further decrease in them of the concentration of free electrons because of recombination.

A change in the shape and position of the perturbation at $t = 0$ showed that the shape and location of the striations at $t \gtrsim t^*$ depend on the initial conditions. Thus, Fig. 3 shows the location of the striations at time $t = 2$ when $\Delta n_e = -0.2$. We see that at the location of the perturbation $\Delta n_e < 0$ a dip in concentration develops. In general we can note that the positive sign of the perturbation $\Delta n_e > 0$ is caused by the development of a striation at the location of the perturbation and, on the other hand, the formation of a "well" in the case $\Delta n_e < 0$. Let us also note that in all calculations the characteristic angle between the average current (axis y) and the striations was approximately 30°-45°.

In the second stage, when $t > t^*$ there is disruption of the striations; these break down into a number of random formations ("tongues," "loops," "bridges," etc.). Figure 4 shows one of the moments of breakdown of the striations shown in Fig. 2. The regions with $n_e > 1$ are cross-hatched. Regular striations become, at $t > t^*$, irregular; in the experiments these are compared with turbulence. A detailed description of irregular structure is given in Section 5.

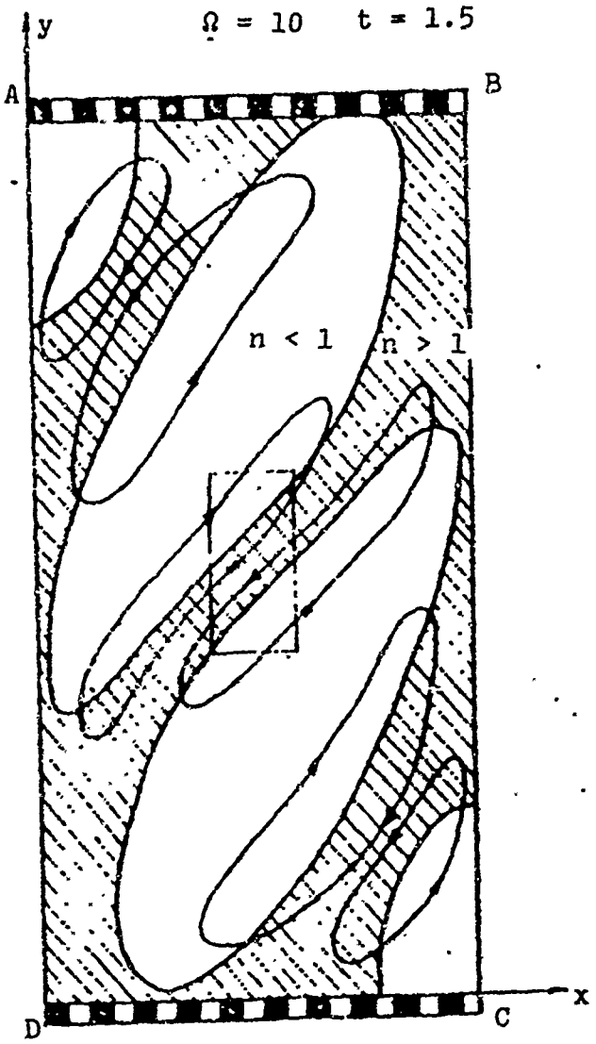

Fig. 2.

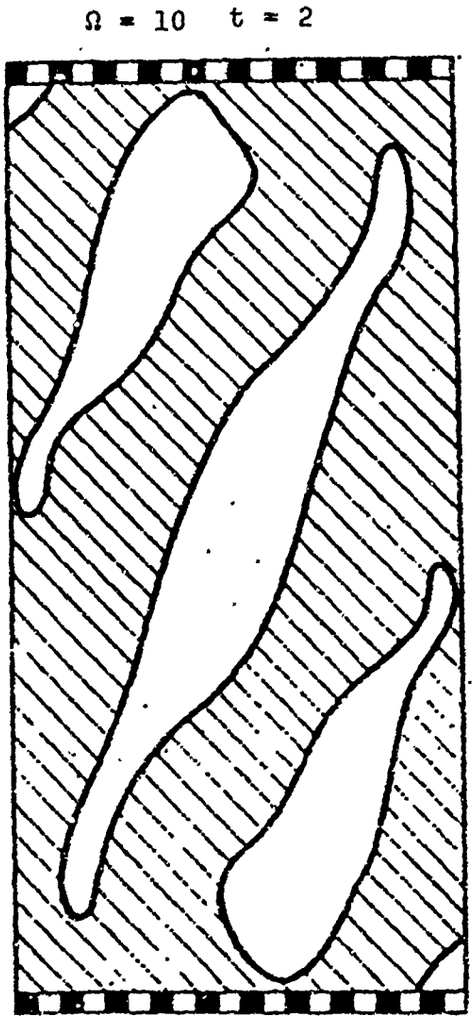

Fig. 3.

$\Omega = 10$ the decay of the central striation occurs at $t \simeq 2$, while for $\Omega = 5$ it occurs at $t \simeq 9.5$. If we arbitrarily assume as t^* the moment of decay of the central striation, the dependence of t^* on Ω is as shown in Fig. 16. When $\Omega = \Omega_{cr} \simeq 3$, the development time t^* tends towards infinity. This means that when $\Omega < \Omega_{cr}$ ionization instability does not develop and no striation formation occurs.

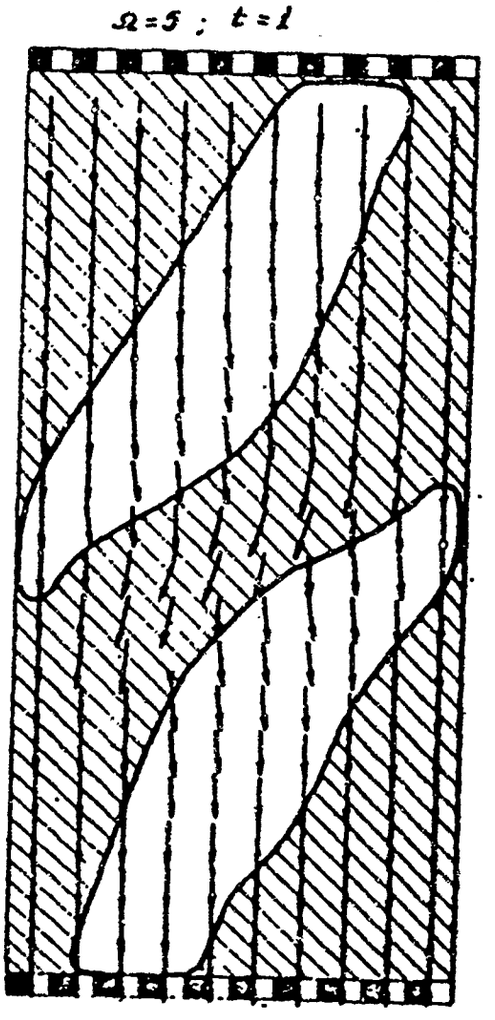

Fig. 6.

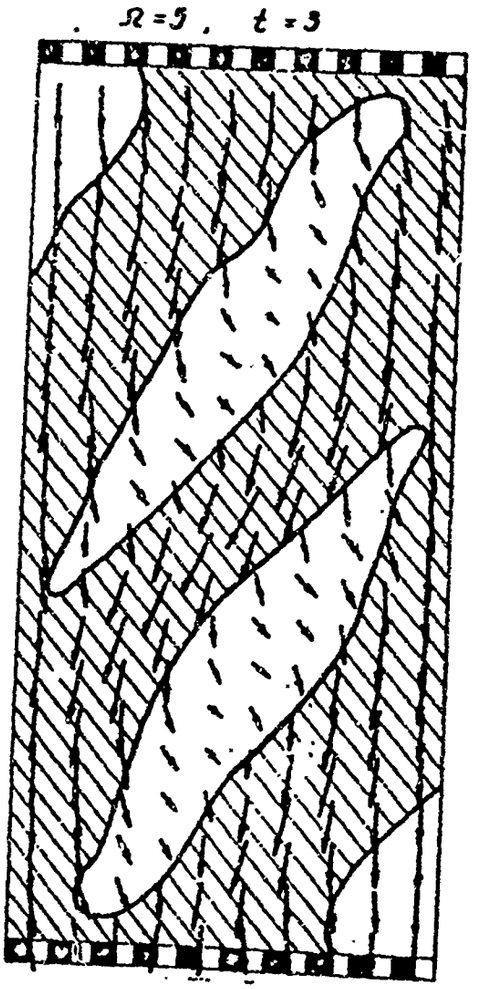

Fig. 7.

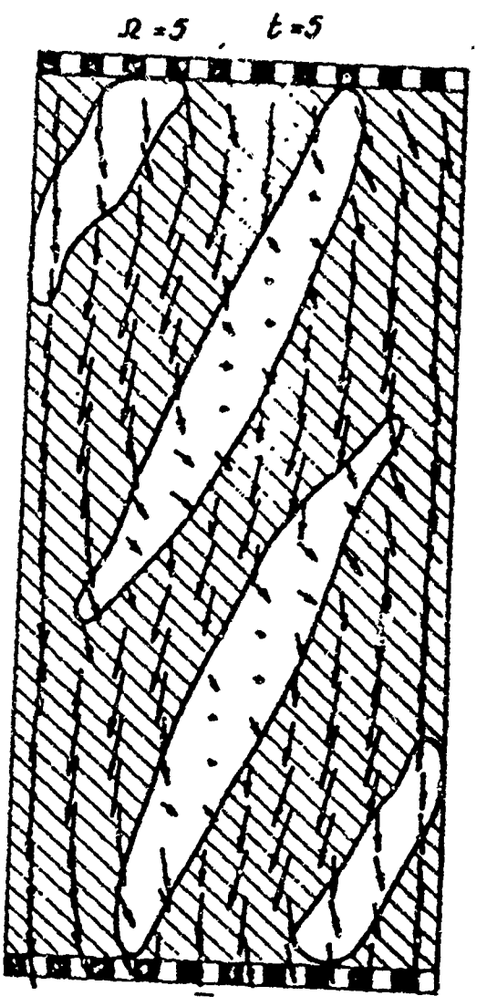

Fig. 8.

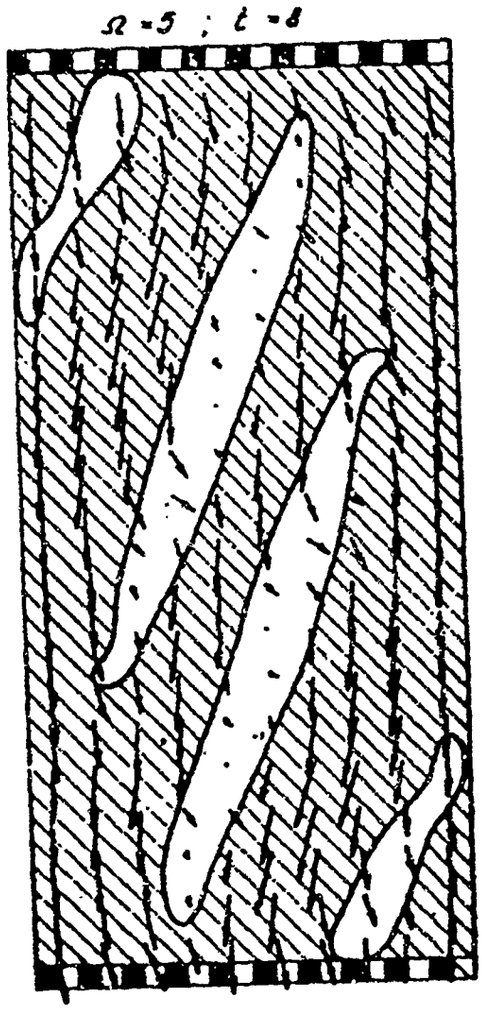

Fig. 9.

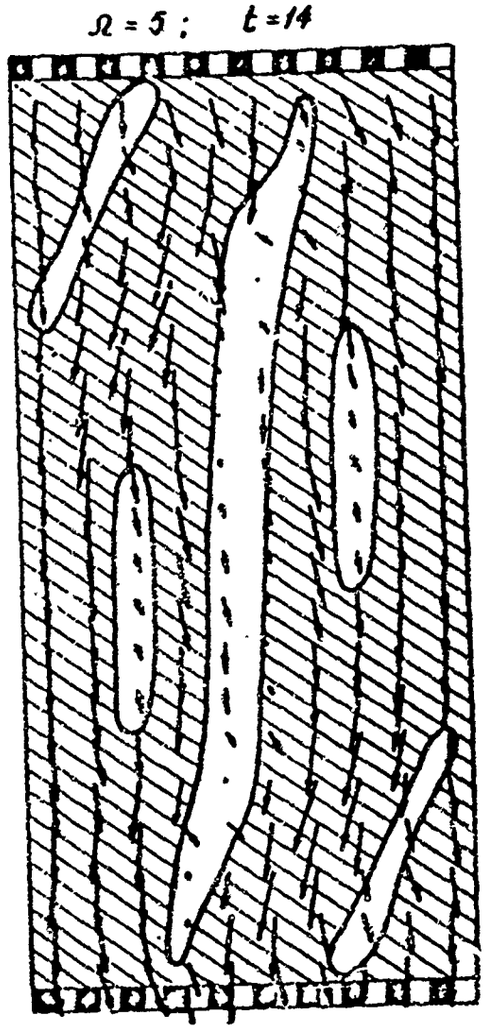

Fig. 10.

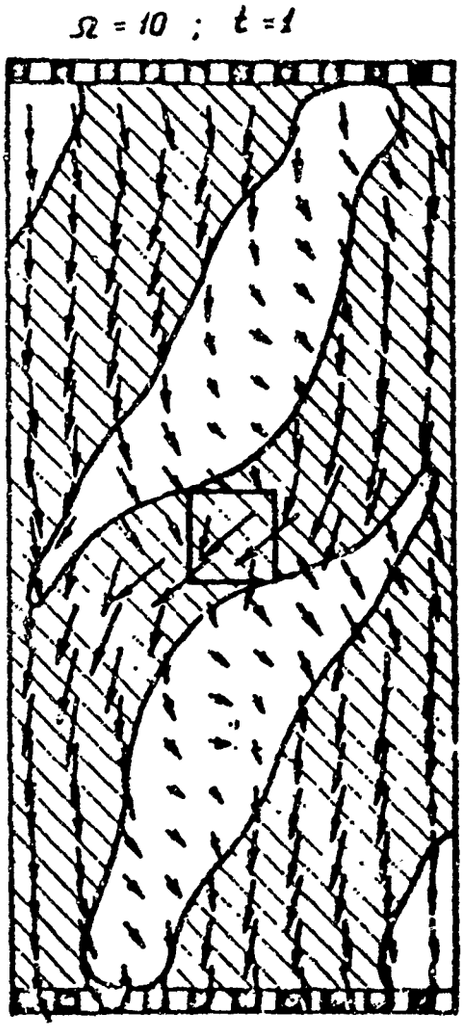

Fig. 11.

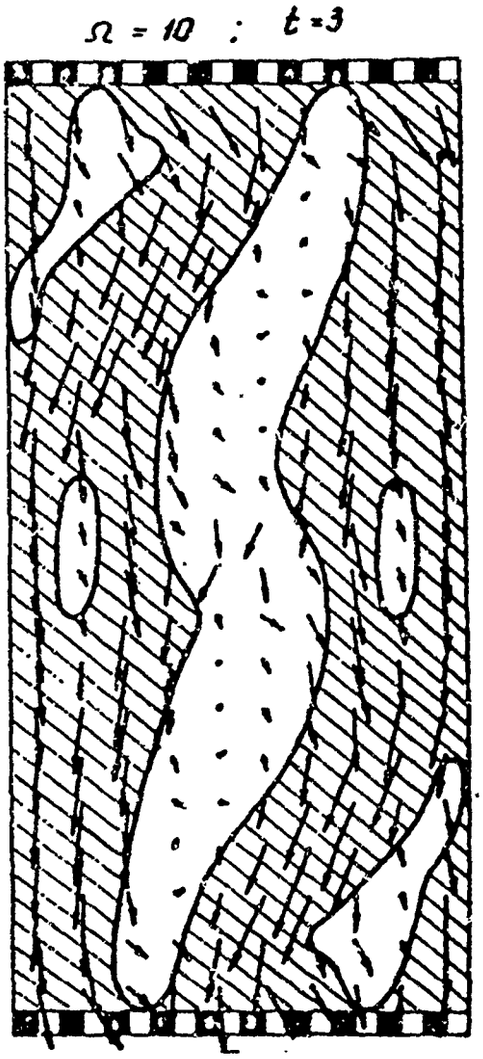

Fig. 12.

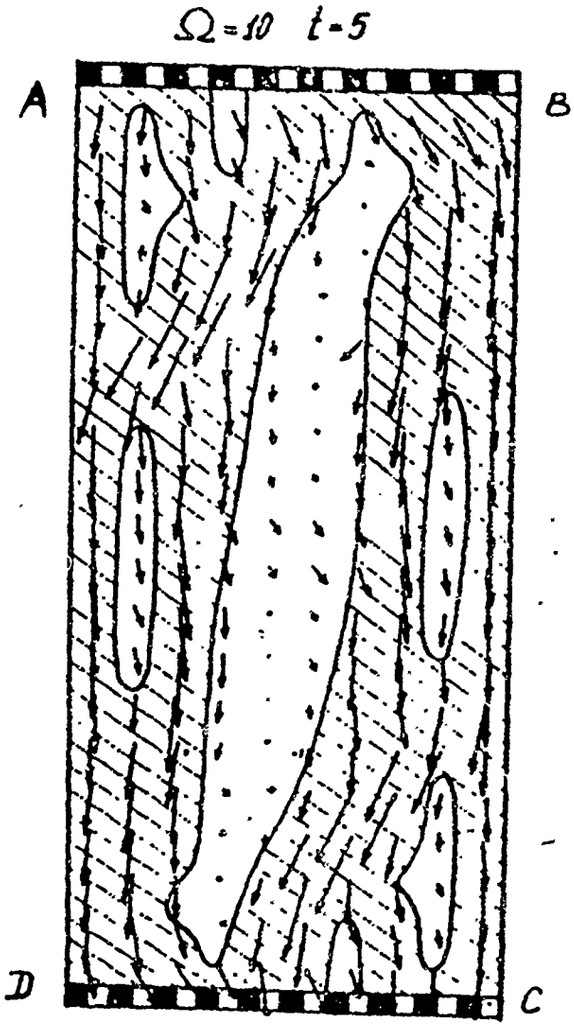

Fig. 13.

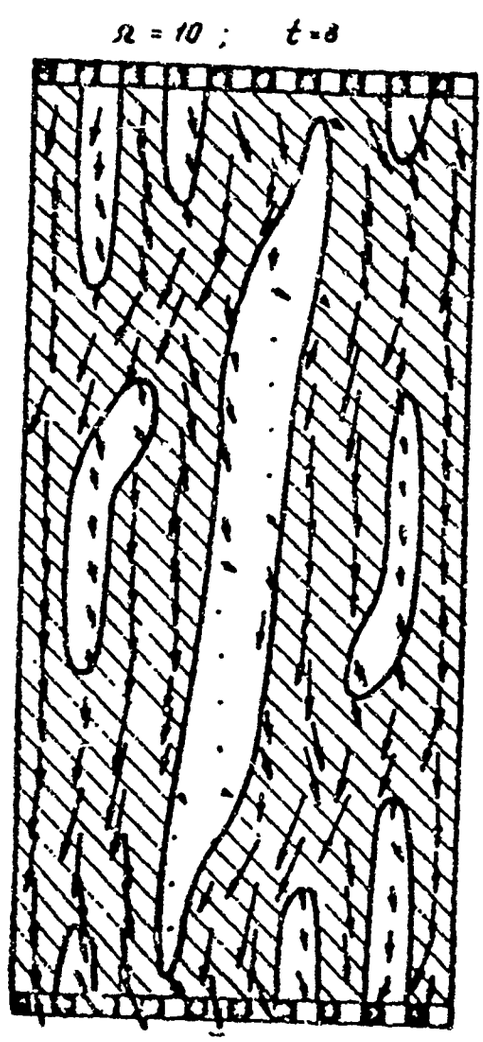

Fig. 14.

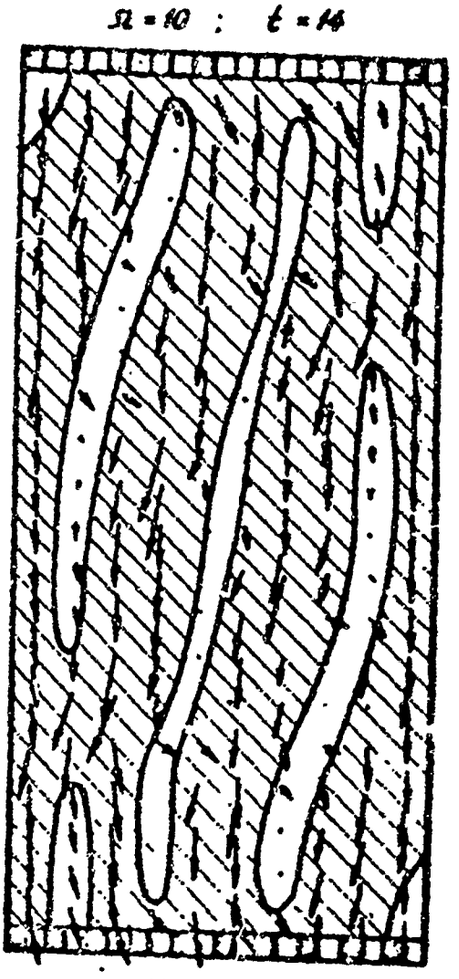

Fig. 15.

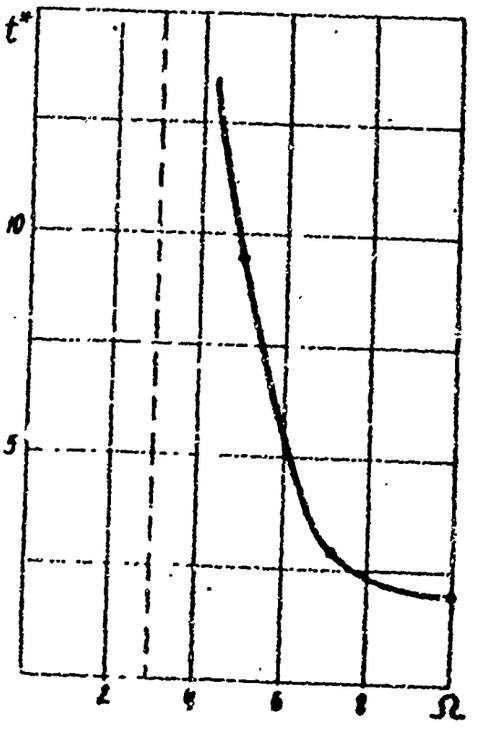

Fig. 16.

Let us turn to an examination of the average values. Figure 17 shows the Hall ratio $\langle E_x \rangle / \langle E_y \rangle$ as a function of time t for various Ω. We should note that the steady-state values $\beta_{eff} = \langle E_x \rangle / \langle E_y \rangle$ do not agree among themselves and, consequently, do not coincide with β_{cr}. This contradicts the hypothesis that $\beta_{eff} > \beta_{cr}$, based on the following reasoning. If $\beta_{eff} > \beta_{cr}$, then in the plasma, as a result of instability, there appear additional nonuniformities which will decrease β_{eff} until its value reaches β_{cr}. Such a foundation is valid, apparently, for small fluctuations on a uniform background. In the developed stage of the process, the fluctuations are not small and the discussion, possibly, becomes inapplicable. Figure 18 shows the steady-state value $\langle E_x \rangle / \langle E_y \rangle$ as $t \to \infty$ as a function of Ω (solid line). From this last graph we see that there is a tendency toward "saturation" of the Hall relationship with an increase in the magnetic field, but the saturation itself occurs when $\Omega/_{t=0} > 10$. Finally, Fig. 19 shows the time variation of σ_{eff} with a parametric change in Ω; Fig. 20 gives the dependence of the steady-state values σ_{eff} as $t \to \infty$ vs. Ω.

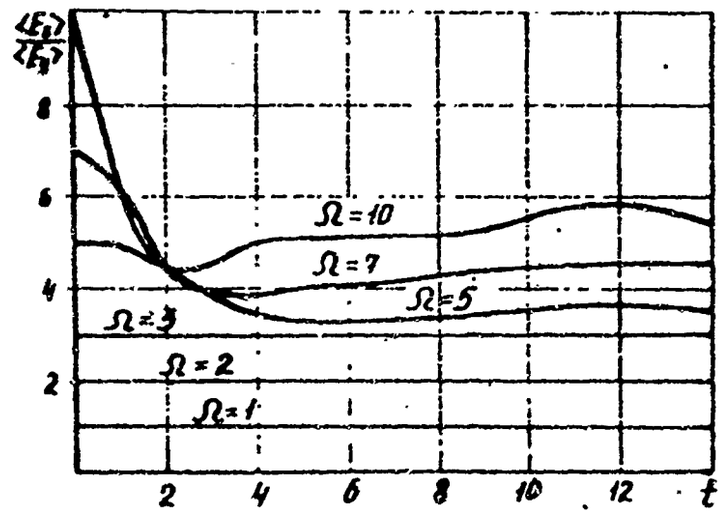

Fig. 17.

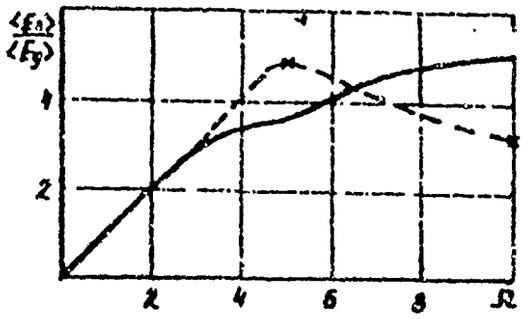

Fig. 18.

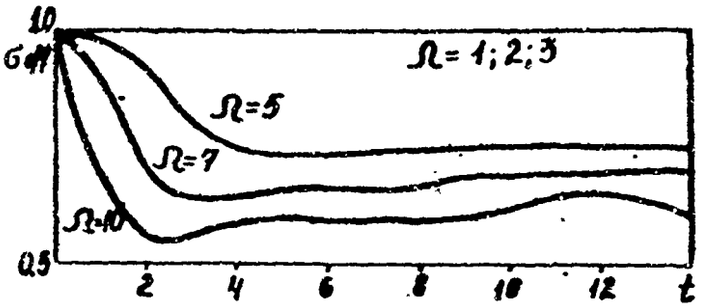

Fig. 19.

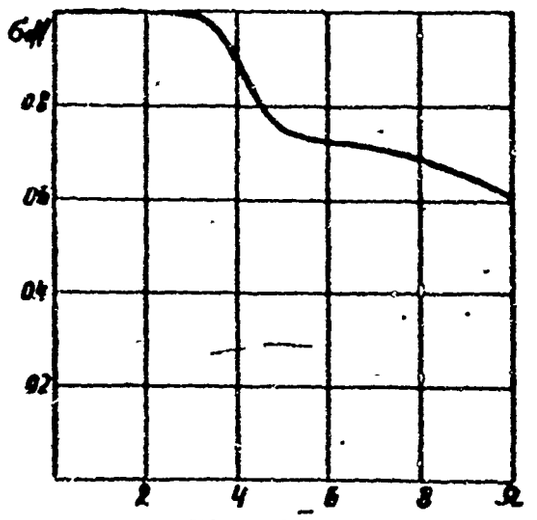

Fig. 20.

1.2. Consideration of collisions of electrons with the neutral component introduces certain qualitative correction. Primarily this relates to the behavior of n_{min} and τ when $t >> t^*$. The value n_{min} when $t \to \infty$ now has a certain limit, while $\langle\tau\rangle$, respectively, stops increasing without limit. This can be seen in Fig. 21, which

corresponds to the case $\Omega = 10$ when $\Delta n_e = 0.2$. The ratio of the initial temperature T_e to the ionization potential I is taken as $k_n = 0.1$. The ratio $A_2/A_1 = 1$, $A_3 = 0$. The lines of level $n_e = 1$ and the field of electric current densities at moment of time t = 1, 5, and 20 are shown in Figs. 22-24.

Calculations were also conducted for other values of Ω. It is characteristic that when taking into account collisions with neutrals, the effect of "saturation" of the Hall ratio with increasing Ω becomes more clearly expressed (Fig. 18, dashed line).

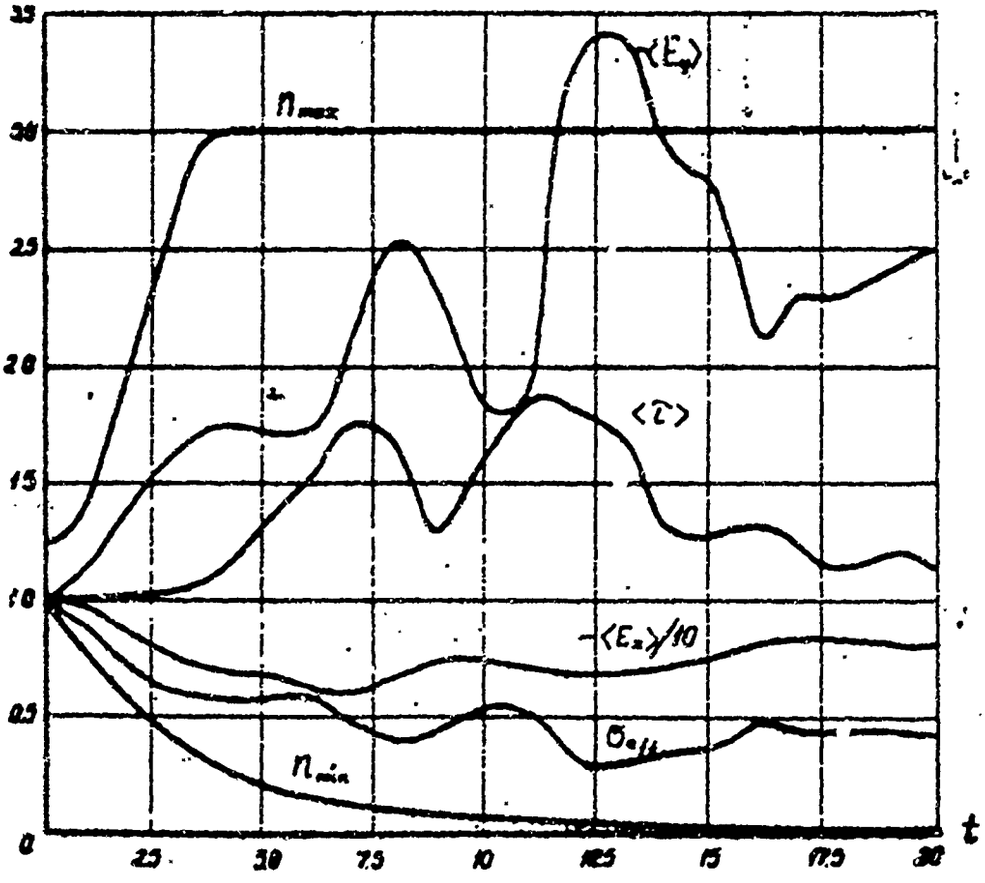

Fig. 21.

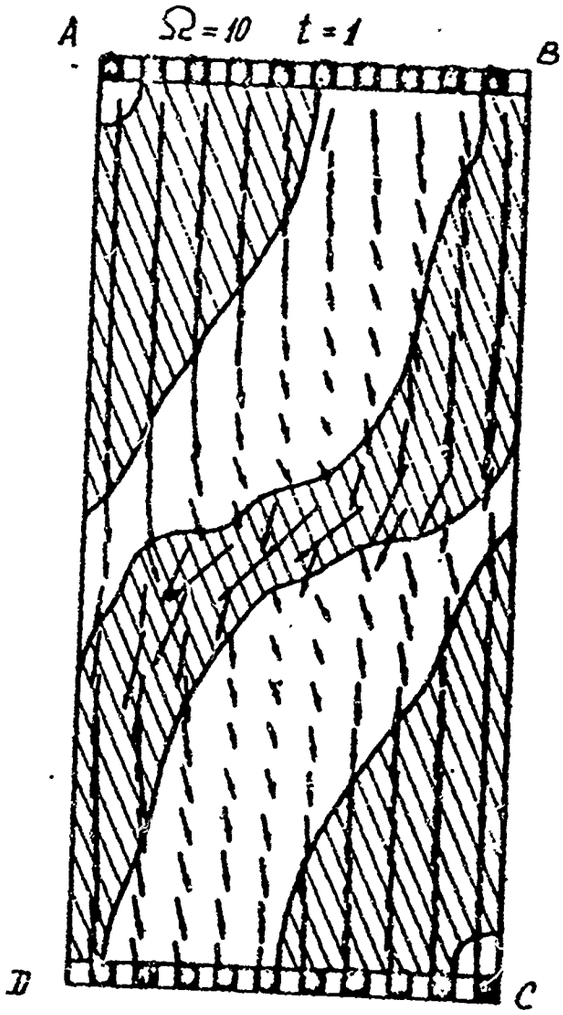

Fig. 22.

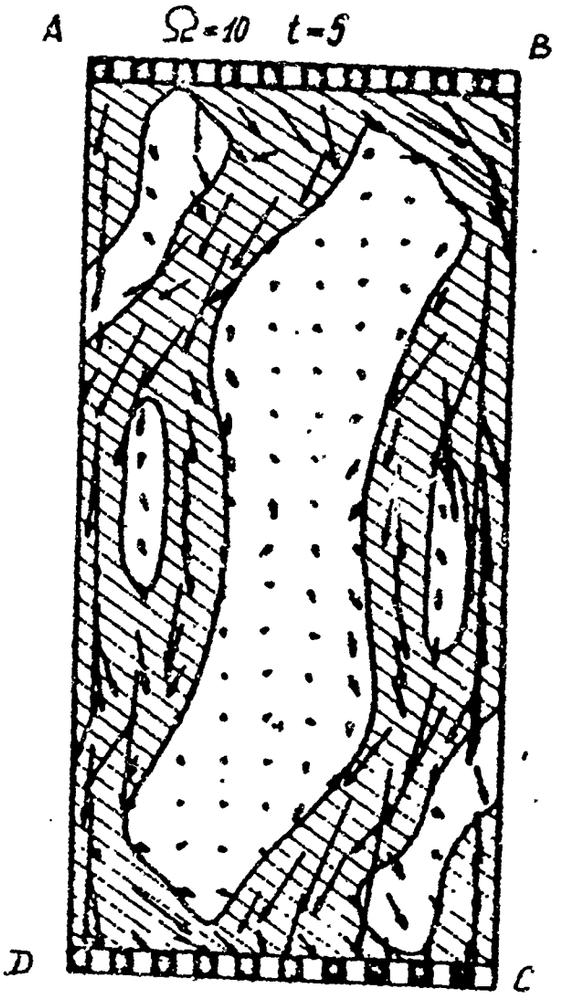

Fig. 23.

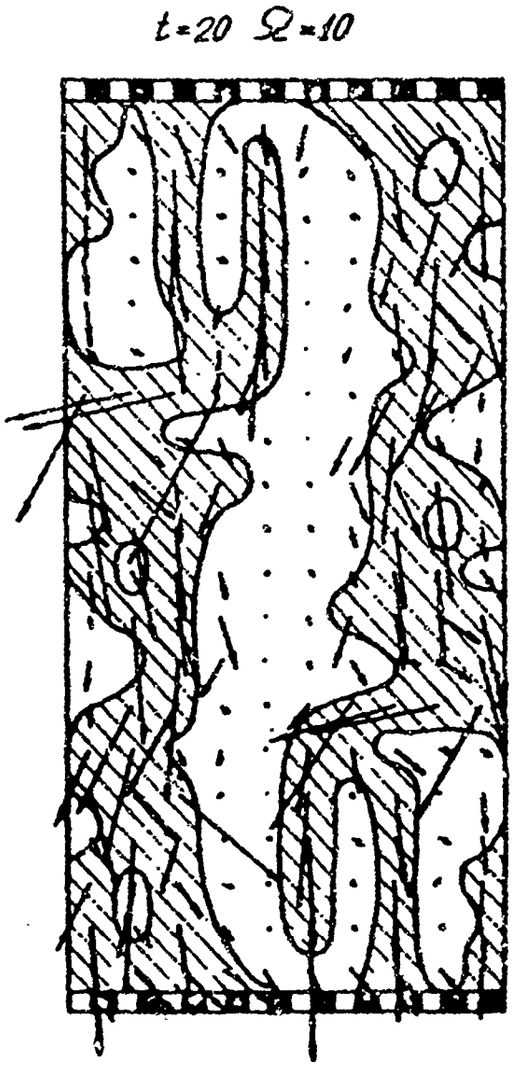

Fig. 24.

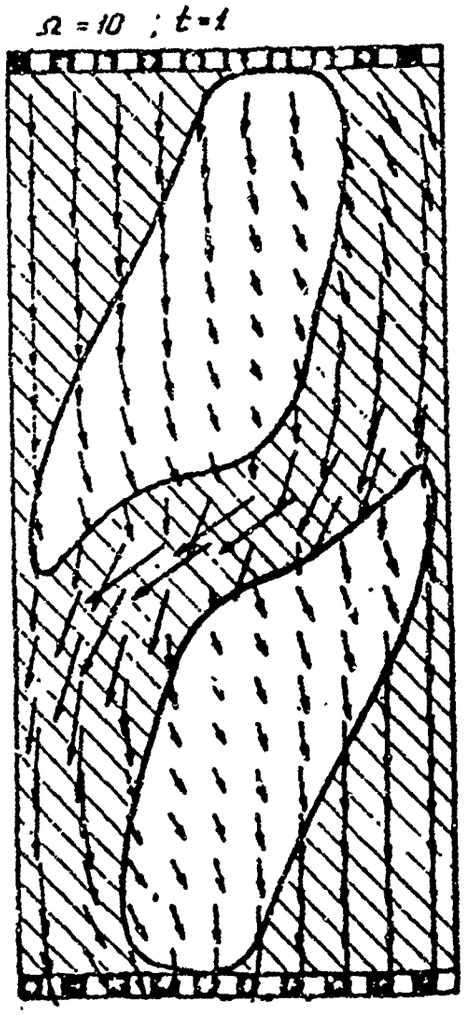

Fig. 25.

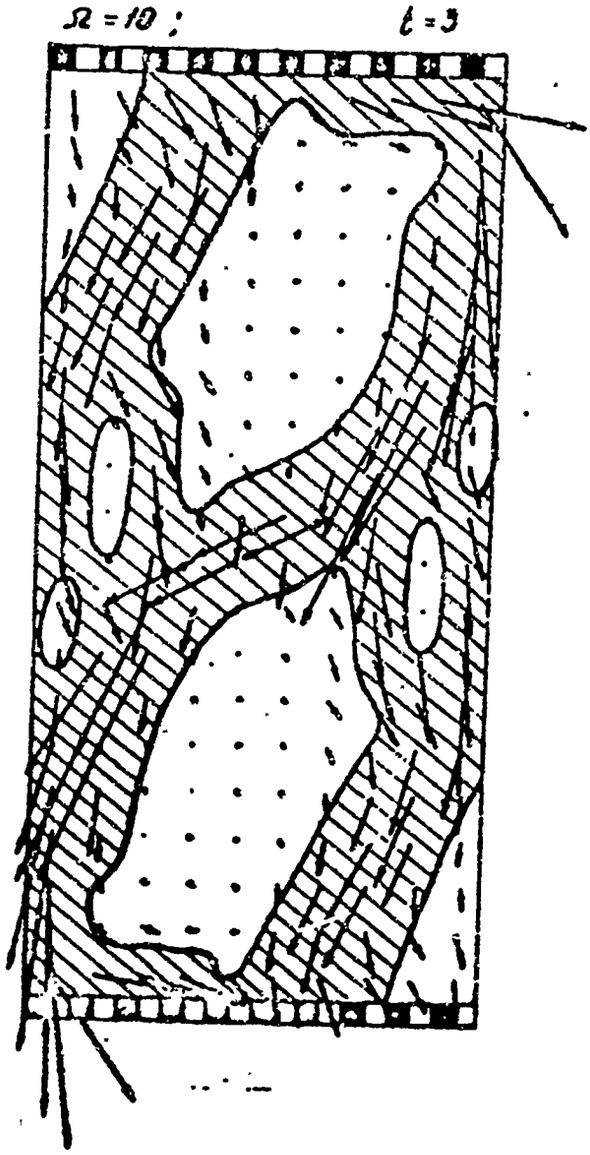

Fig. 26.

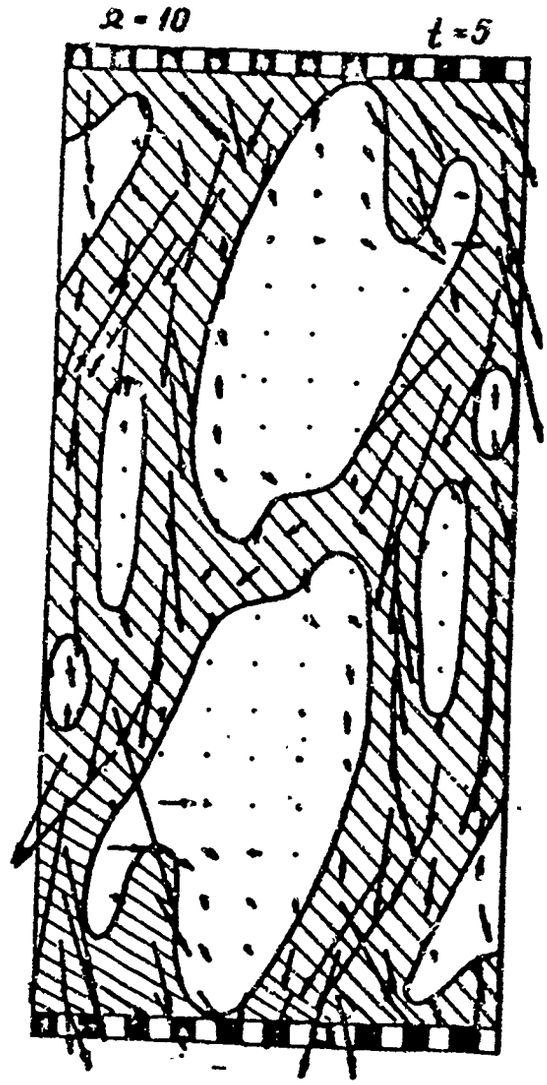

Fig. 27.

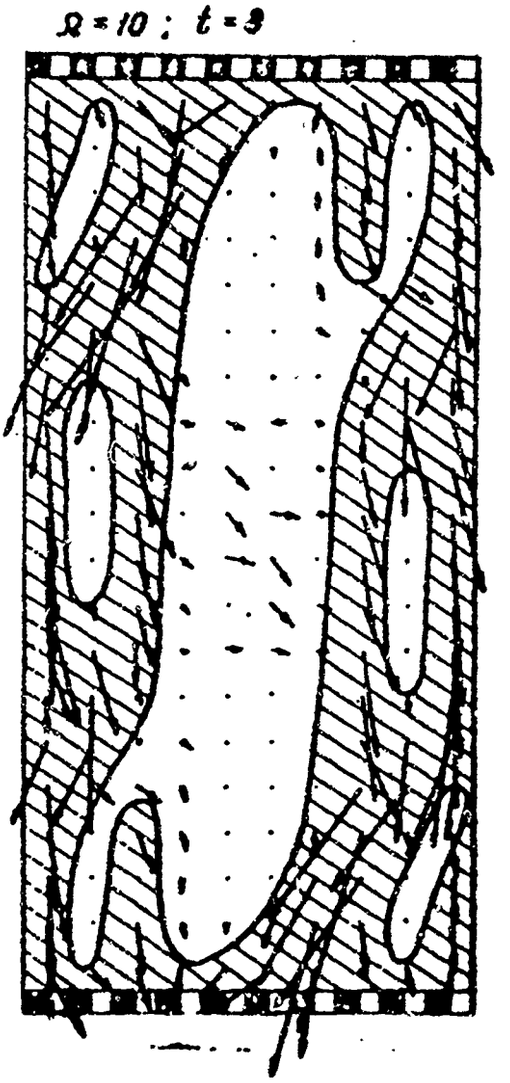

Fig. 28.

For an explanation of the influence of degree of ionization of the plasma on the nature of the development of ionization instability we perform calculations for various ratios of A_2/A_1. Figures 25-28 show the results of a numerical solution of a version analogous to that examined above but with $A_2/A_1 = 10$, i.e., in the case of a weakly-ionized plasma. We can note that the process of development of striations occurs somewhat more slowly than when $A_2/A_1 = 1$. The qualitative dependence of t^* on A_2/A_1 when $\Omega = 10$ is shown in Fig. 29.

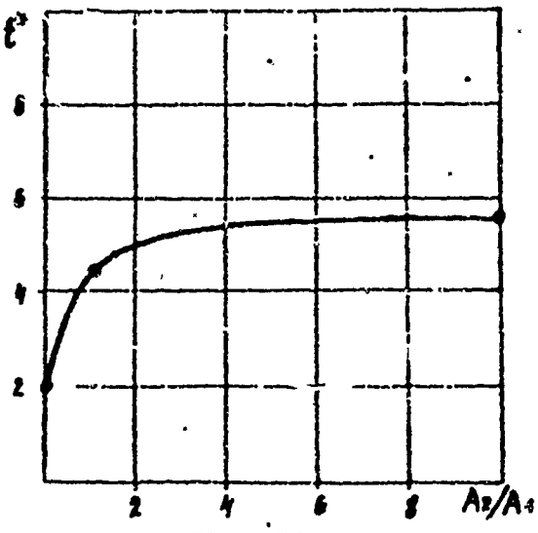

Fig. 29.

2. Let us change the statement of the problem as follows. Let us assume that the dielectric walls are spaced farther apart, while the ideally sectioned electrodes ab = 1 and cd = 1 are located right in the middle. Sections Aa, bB, Cc, and dD are ideal dielectrics. The current density on the electrodes of the process is given as $j_y = -1$. The number of cells N = 600 (h = 0.1). Otherwise, the statement is as in section 1. Let us note that there is as yet no need to introduce perturbation into the initial conditions, since there is no trivial solution.

2.1. Coulomb plasma. Figures 30-34 show the lines of the level and the vector field of the electric current density for $\Omega = 10$ and times t = 1, 1.8, 3, 7, and 18.2.

At the initial moment of time the electron concentration is uniform; therefore the electric current field is perturbed only by the Hall effect. Near the electrodes the current density is highest; here regions of increased concentration n_e are formed. Consequently, the effective Hall parameter here abruptly decreases, while the currents "approach" in direction the vector of the average electric field and flow primarily along the electrodes. Powerful current layers are formed which depart from the electrodes and propagate along the dielectric portions Aa and Cc (Fig. 30). Within the layers there is intense plasma ionization. Near the points b and c the electron concentration rapidly increases and reaches a limiting value.

Because Ω is finite, the currents from the layers are diffused and directed toward opposite electrodes.

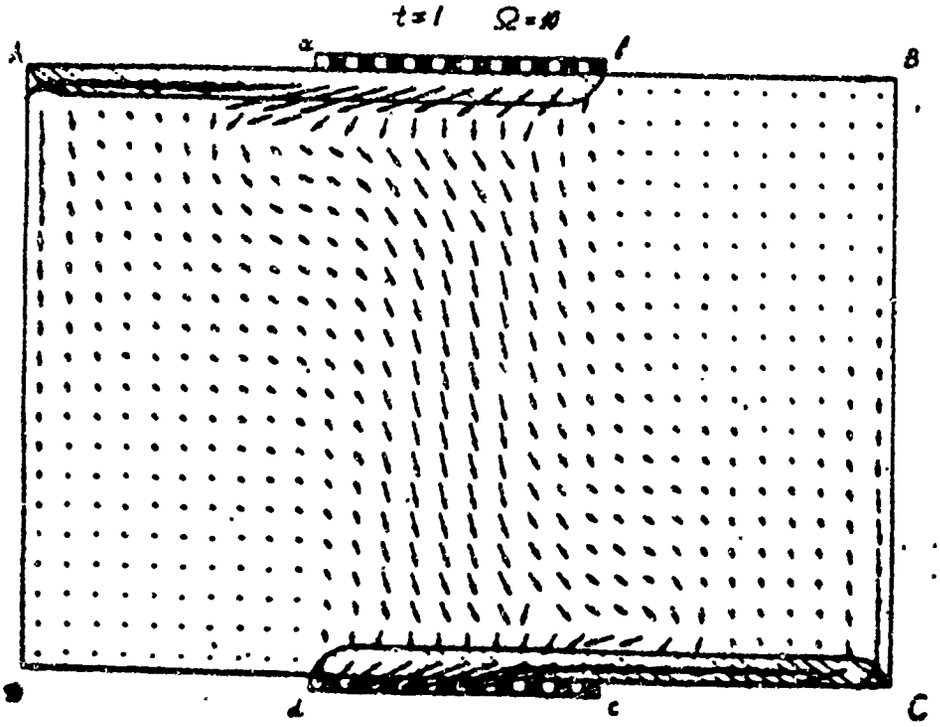

Fig. 30.

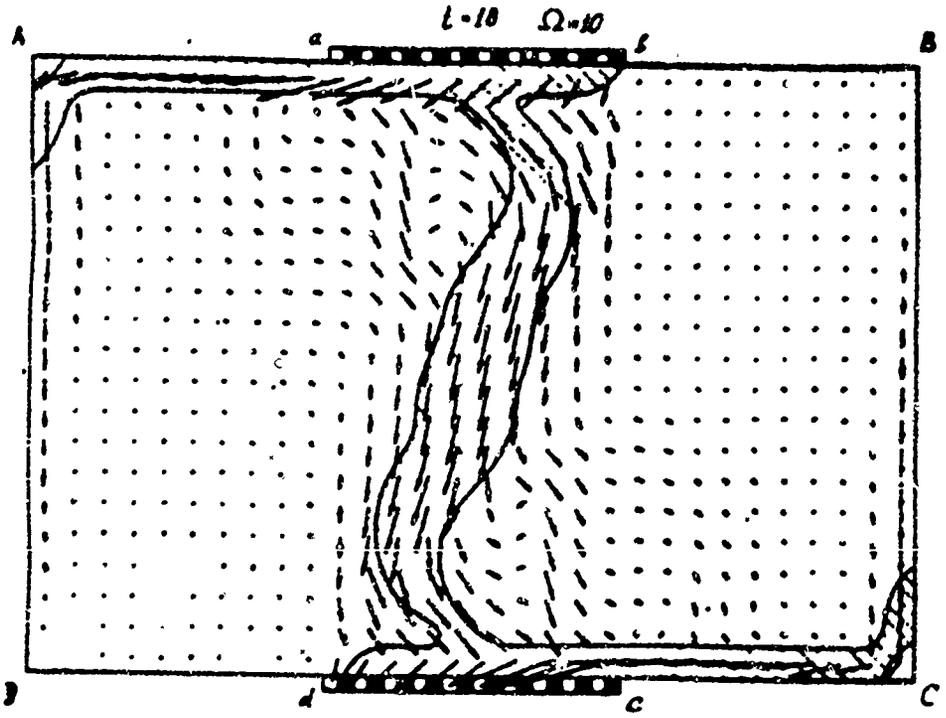

Fig. 31.

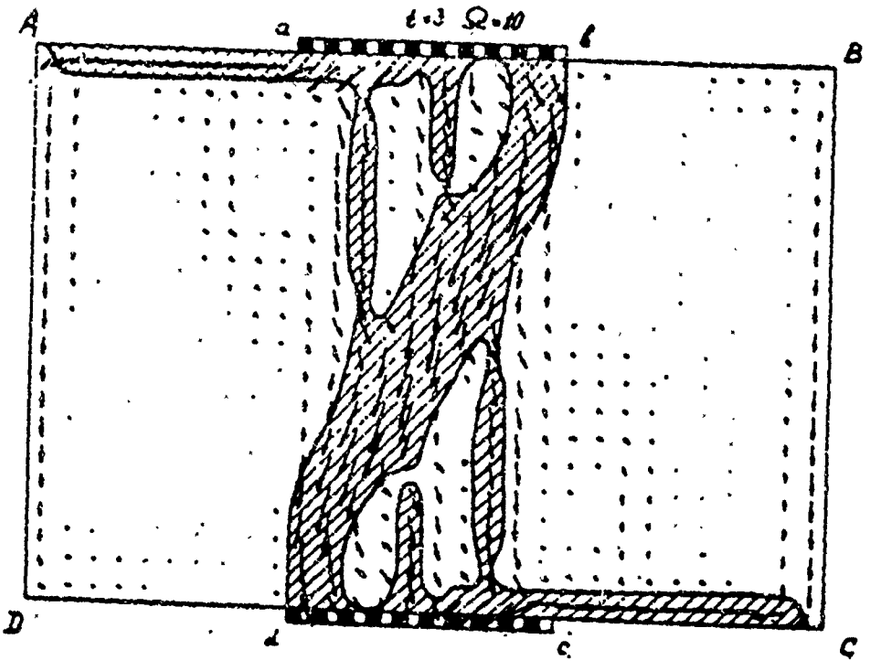

Fig. 32.

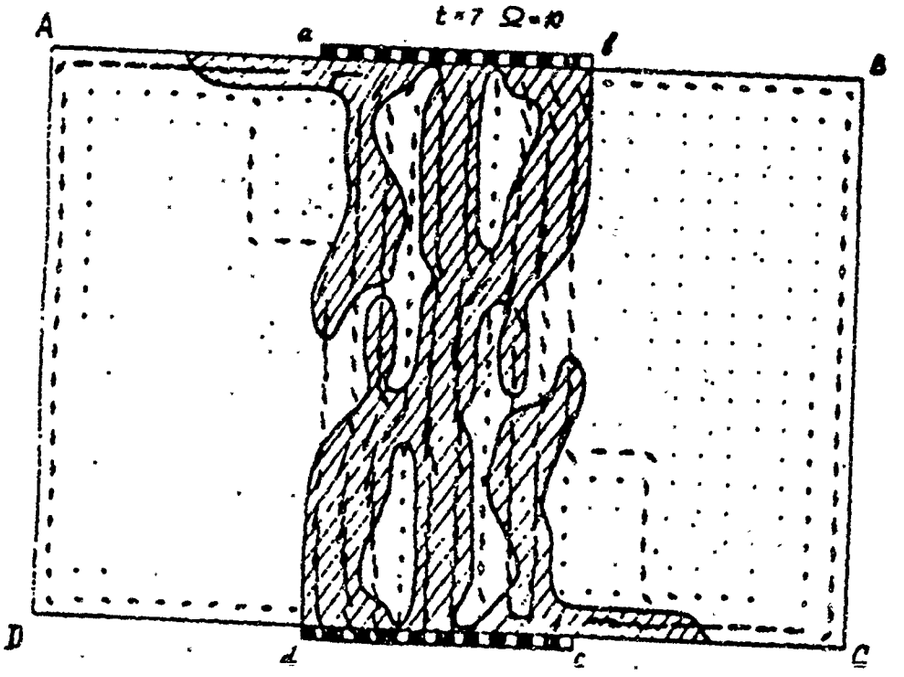

Fig. 33.

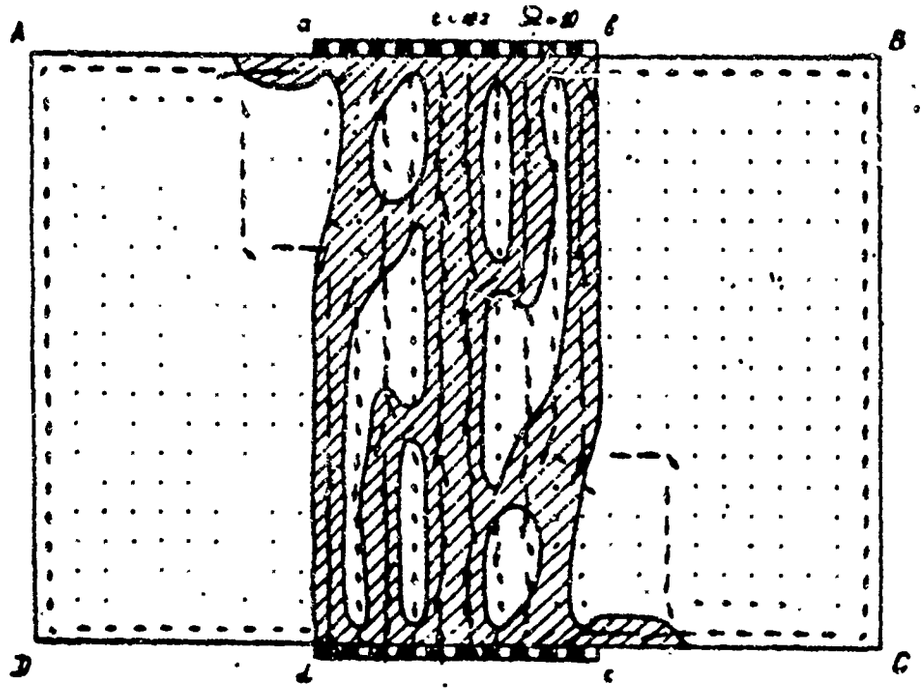

Fig. 34.

After a certain time (Fig. 31), between the electrodes there appears a region of increased ionization (striation) along which the electric current contracts and there is intense release of Joule heat, causing an increase in concentration n_e. The maximum concentrations n_e about points b and c decreases somewhat, since an ever increasing considerable part of the current tends from the electrodes along the striation. This drop in n_{max} is shown in Fig. 35, where, in addition to n_{max} and n_{min}, there are depicted the average and effective values as functions of time. The point of maximum concentration appears to lie within the striation.

In the second stage, when $t > t^*$ (for the given variant $t^* \gtrsim 5$), the striation breaks down into several current pinches located almost vertical from electrode to electrode. Approximately the same picture is observed during experimental study of striations on finitely sectioned electrodes.

As before, the transition from the second stage is accompanied by the establishment of average values (excluding $\langle\tau\rangle$ and n_{min}), despite the absence of stable stationary distribution of n_e and the electric

current field. The asymptotic value of $\langle E_x \rangle / \langle E_y \rangle$ at $t \to \infty$ became equal to 3.3 for $\Omega = 10$ instead of the value of 5.5 given in Section 2, while σ_{eff} in this case tends towards 0.35.

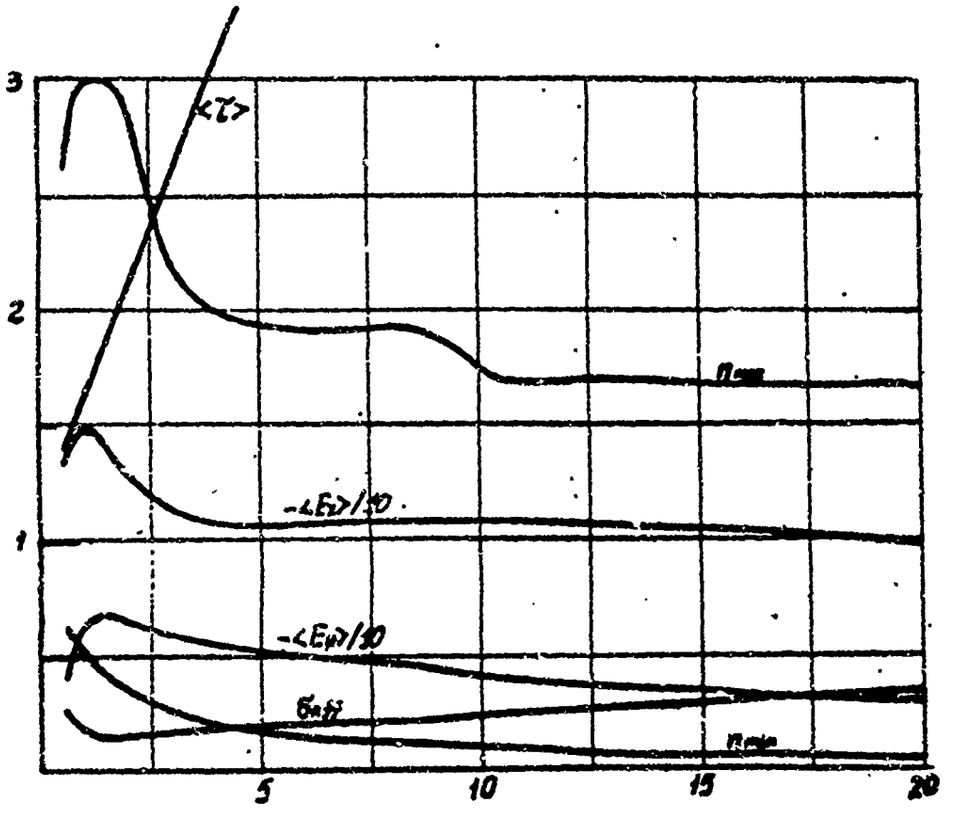

Fig. 35.

Calculations performed for various values of Ω showed that the appearance of ionization instability begins at $\Omega_{cr} \simeq 3$.

2.2. Consideration of collisions of electrons with neutrals, just as in the problem of Section 1.2, leads to asymptotic establishment of $\langle \tau \rangle$ and n_{min}. We can also again point out the slower transition to the second stage of "pinching" of the currents and decay of the striations. The results of numerical solution of the problem of Section 2.1, with consideration of collisions of electrons and neutrals at $\Omega = 10$ and $A_2/A_1 = 1$, are given in Figs. 36-38 for times $t = 1$, 5, and 8.

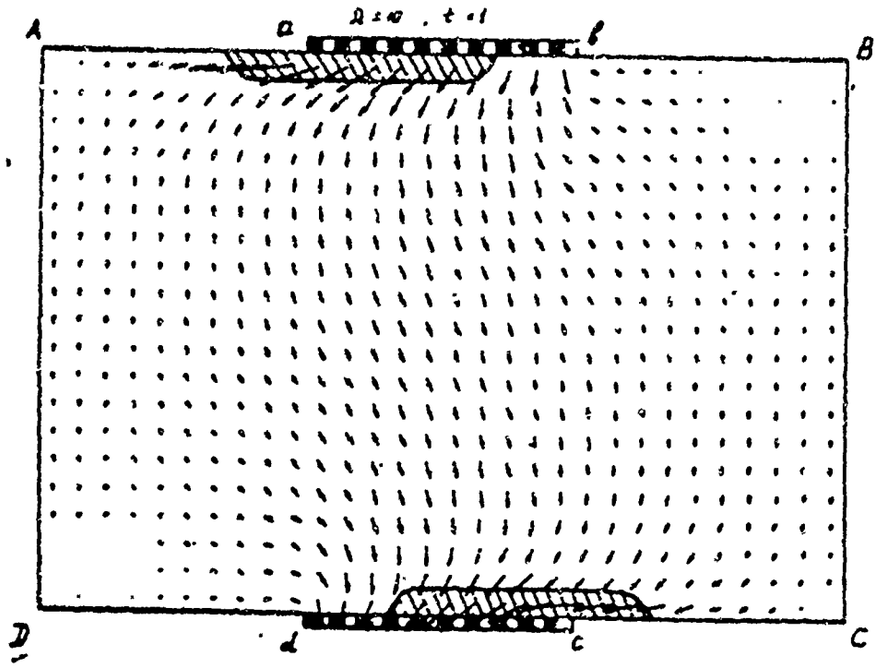

Fig. 36.

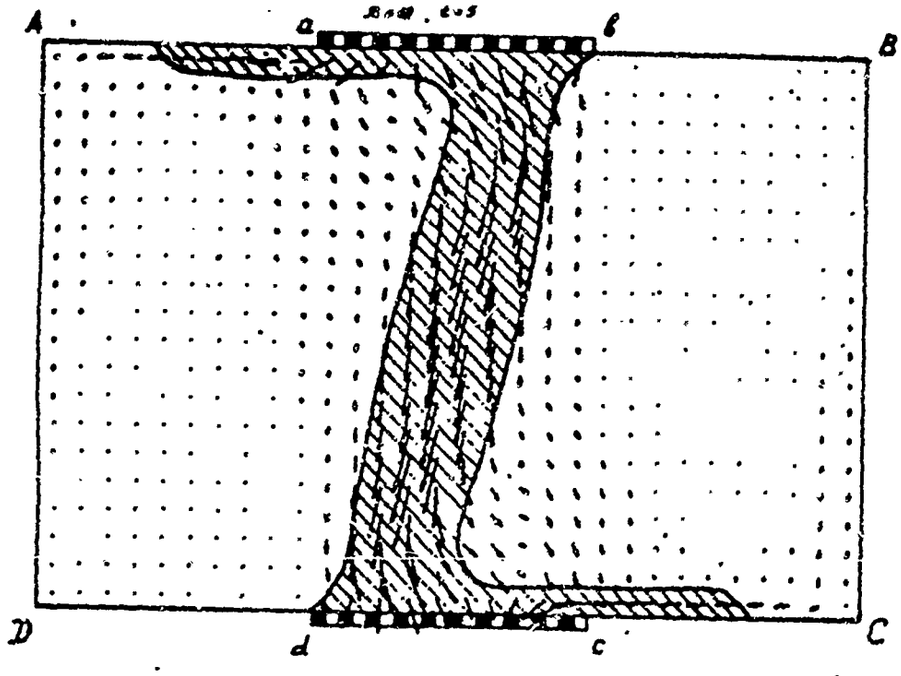

Fig. 37.

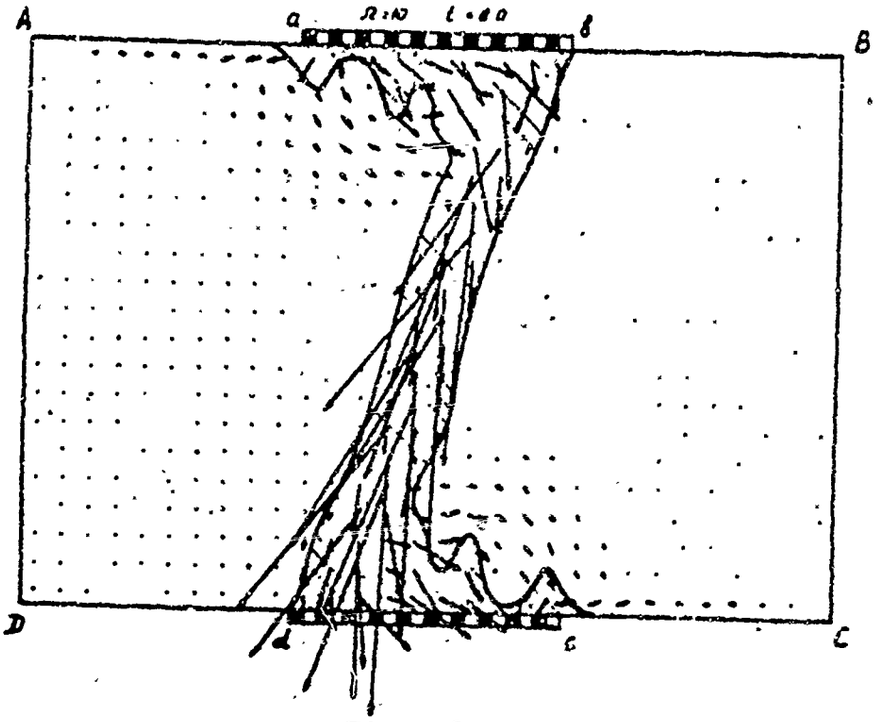

Fig. 38.

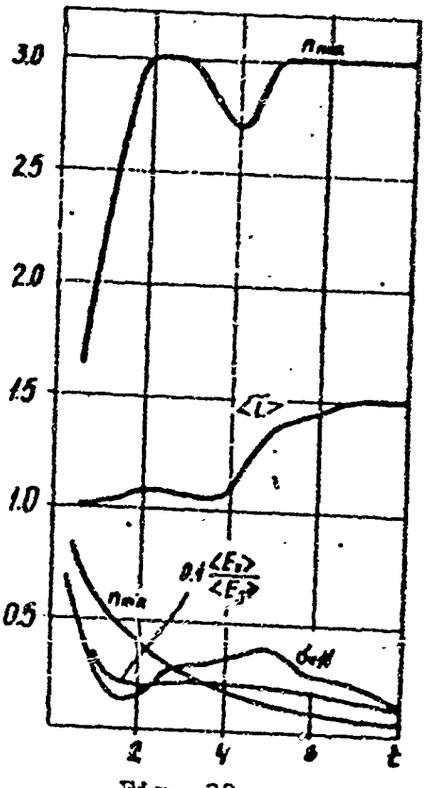

Fig. 39.

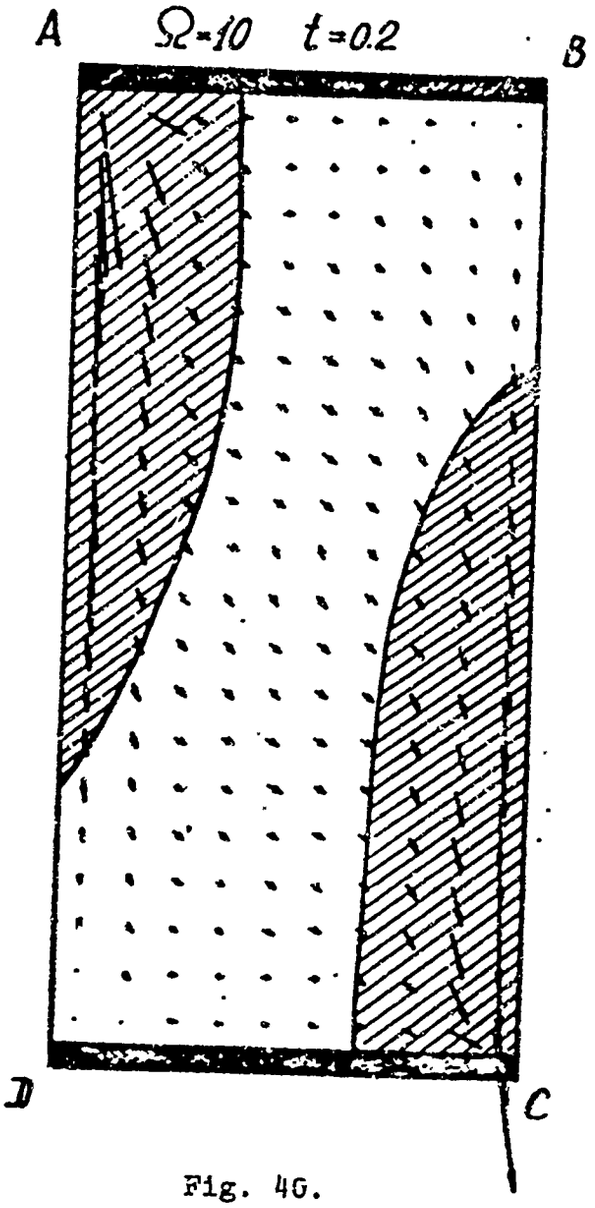

Fig. 40.

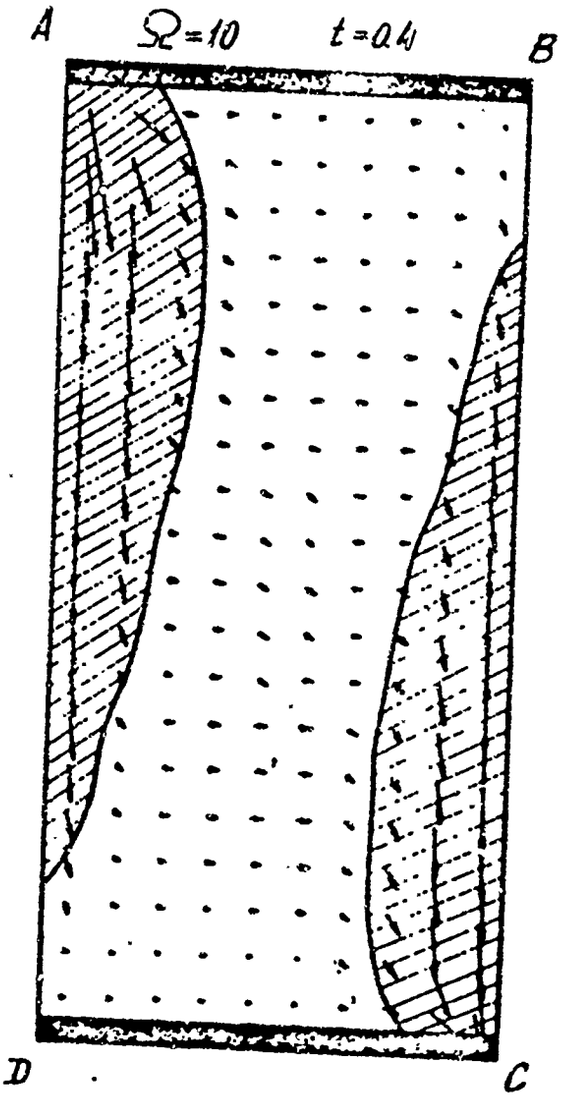

Fig. 41.

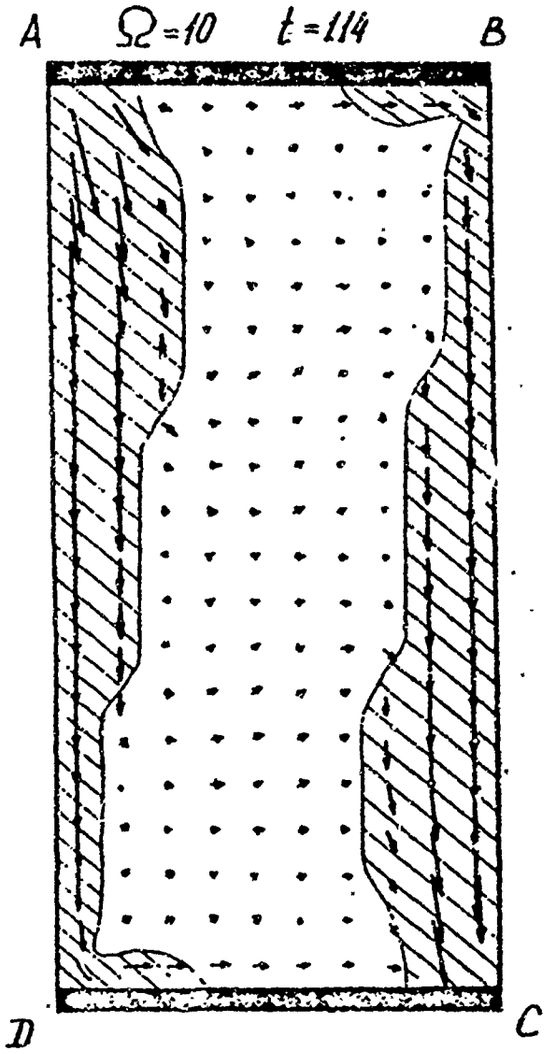

Fig. 42.

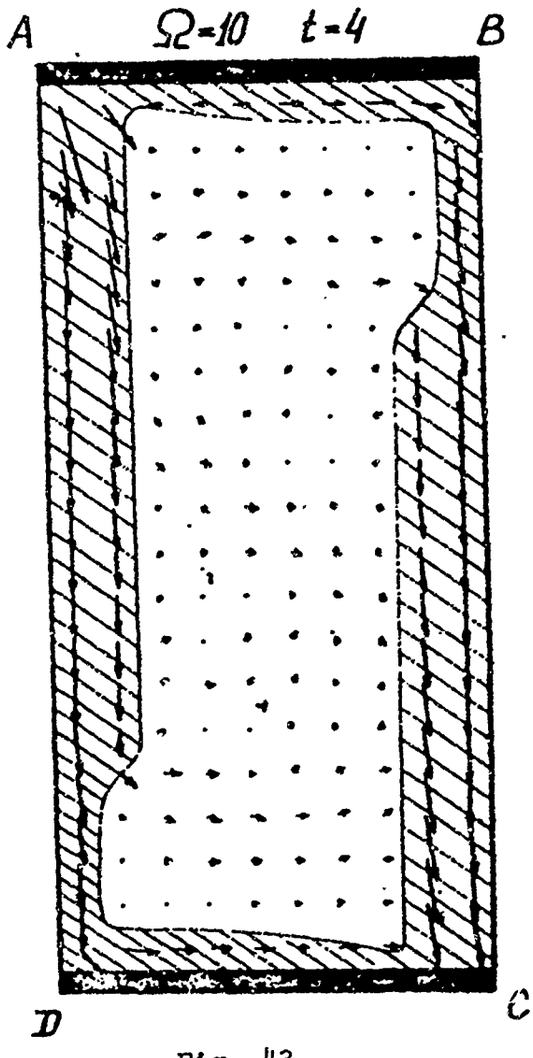

Fig. 43.

The time variation of effective and average values is shown in Fig. 39. Let us note that the dip in n_{max} occurring during the striation formation process then disappears, unlike the case of Coulomb plasma.

3. Let us examine the interaction of nonequilibrium ionized plasma with solid ideally conducting electrodes. Here we limited ourselves to the case of Coulomb plasma $\sigma = 1$.

3.1. First let us examine a statement of the problem similar to that in Section 1. At the initial moment $t = 0$, j_x, j_y, and n_e are uniformly distributed in space with values $j_x = 0$, $j_y = -1$, and $n_e = 1$. An external magnetic field is applied to the entire volume ABCD (AB = CD = 1, AD = BC = 2), and its value is such that at the initial moment of time the Hall parameter $\Omega_0 = 10$. The horizontal section AB and CD of the boundary of the region (see Fig. 1) are solid ideally conducting electrodes instead of ideally sectioned electrodes examined in Section 1.

Figures 40-43 show the three-dimensional distribution of the electric current density components j_x, j_y and electron concentration n_e, respectively, for times $t = 0.2$, 0.4, 1.14, and 4.0.

Let us remember that for the problem examined in Section 1 the initial data $j_x = 0$, $j_y = -1$, $n_e = 1$ are the steady-state solution. In the problem with solid electrodes such values of j_x, j_y, and n_e satisfy the equations, but do not satisfy the boundary conditions on the solid electrodes: $j_x = -\Omega j_y$. Therefore here there is no need to introduce perturbations into the initial data in order to initiate the nonstationary process. In the initial stage, because of the strong Hall effect ($\Omega = 10$), the current is concentrated on the left end of the upper electrode AB (point A = a) and on the right end of the lower electrode CD (at point C = c). Corresponding to this, in the upper left and lower right corners of the region there is localization of Joule heating, which leads to increased ionization of plasma and the achievement, at $t = 0.2$, of maximum electron concentration

The time variation of effective and average values is shown in Fig. 39. Let us note that the dip in n_{max} occurring during the striation formation process then disappears, unlike the case of Coulomb plasma.

3. Let us examine the interaction of nonequilibrium ionized plasma with solid ideally conducting electrodes. Here we limited ourselves to the case of Coulomb plasma $\sigma = 1$.

3.1. First let us examine a statement of the problem similar to that in Section 1. At the initial moment $t = 0$, j_x, j_y, and n_e are uniformly distributed in space with values $j_x = 0$, $j_y = -1$, and $n_e = 1$. An external magnetic field is applied to the entire volume ABCD (AB = CD = 1, AD = BC = 2), and its value is such that at the initial moment of time the Hall parameter $\Omega_0 = 10$. The horizontal section AB and CD of the boundary of the region (see Fig. 1) are solid ideally conducting electrodes instead of ideally sectioned electrodes examined in Section 1.

Figures 40-43 show the three-dimensional distribution of the electric current density components j_x, j_y and electron concentration n_e, respectively, for times $t = 0.2$, 0.4, 1.14, and 4.0.

Let us remember that for the problem examined in Section 1 the initial data $j_x = 0$, $j_y = -1$, $n_e = 1$ are the steady-state solution. In the problem with solid electrodes such values of j_x, j_y, and n_e satisfy the equations, but do not satisfy the boundary conditions on the solid electrodes: $j_x = -\Omega j_y$. Therefore here there is no need to introduce perturbations into the initial data in order to initiate the nonstationary process. In the initial stage, because of the strong Hall effect ($\Omega = 10$), the current is concentrated on the left end of the upper electrode AB (point A = a) and on the right end of the lower electrode CD (at point C = c). Corresponding to this, in the upper left and lower right corners of the region there is localization of Joule heating, which leads to increased ionization of plasma and the achievement, at $t = 0.2$, of maximum electron concentration

n_e = 3 (Fig. 40). Beginning at moment t $\approx$ 1 (Fig. 41) the regions of increased electron concentration (n_e > 1) are propagated along the vertical sections of boundaries AD and CB, forming along them layers of increased concentration n_e, while in the center of the region the electron density drops. The current passes primarily along these layers, passing between them and agitating the plasma in the center of the region (Fig. 42). By time t = 4 (Fig. 43) the layer of increased electron concentration has extended along the entire boundary of the region, while inside on the background of electron concentration $n_e \approx 0.5$, the current density is low in comparison with the density on the boundary, and is randomly distributed in space. Thus, the local nature of distribution j_x, j_y, and n_e in space differs substantially from the nature of the distribution with ideally sectioned electrodes (see Figs. 2-4). This leads to a substantial difference in the integral characteristics (cf. Fig. 5 and Fig. 44). The establishment of magnitudes $\langle E_x \rangle / \langle E_y \rangle$, and σ_{eff} with time here occurs by the time t = 1, i.e., considerably sooner than in the case of ideally sectioned electrodes. Turbulent resistance is greater by a factor of 2.5, while the ratio $\langle E_x \rangle / \langle E_y \rangle$ is an order of magnitude smaller.

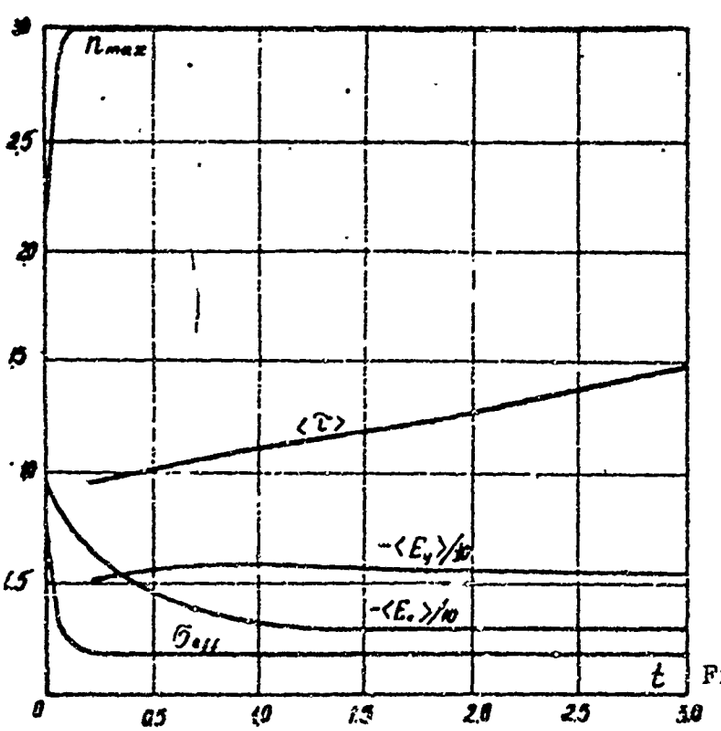

Fig. 44.

$n_e \approx 3$ (Fig. 40). Beginning at moment $t \approx 1$ (Fig. 41) the regions of increased electron concentration ($n_e > 1$) are propagated along the vertical sections of boundaries AD and CB, forming along them layers of increased concentration n_e, while in the center of the region the electron density drops. The current passes primarily along these layers, passing between them and agitating the plasma in the center of the region (Fig. 42). By time $t = 4$ (Fig. 43) the layer of increased electron concentration has extended along the entire boundary of the region, while inside on the background of electron concentration $n_e \approx 0.5$, the current density is low in comparison with the density on the boundary, and is randomly distributed in space. Thus, the local nature of distribution j_x, j_y, and n_e in space differs substantially from the nature of the distribution with ideally sectioned electrodes (see Figs. 2-4). This leads to a substantial difference in the integral characteristics (cf. Fig. 5 and Fig. 44). The establishment of magnitudes $\langle E_x \rangle / \langle E_y \rangle$, and σ_{eff} with time here occurs by the time $t = 1$, i.e., considerably sooner than in the case of ideally sectioned electrodes. Turbulent resistance is greater by a factor of 2.5, while the ratio $\langle E_x \rangle / \langle E_y \rangle$ is an order of magnitude smaller.

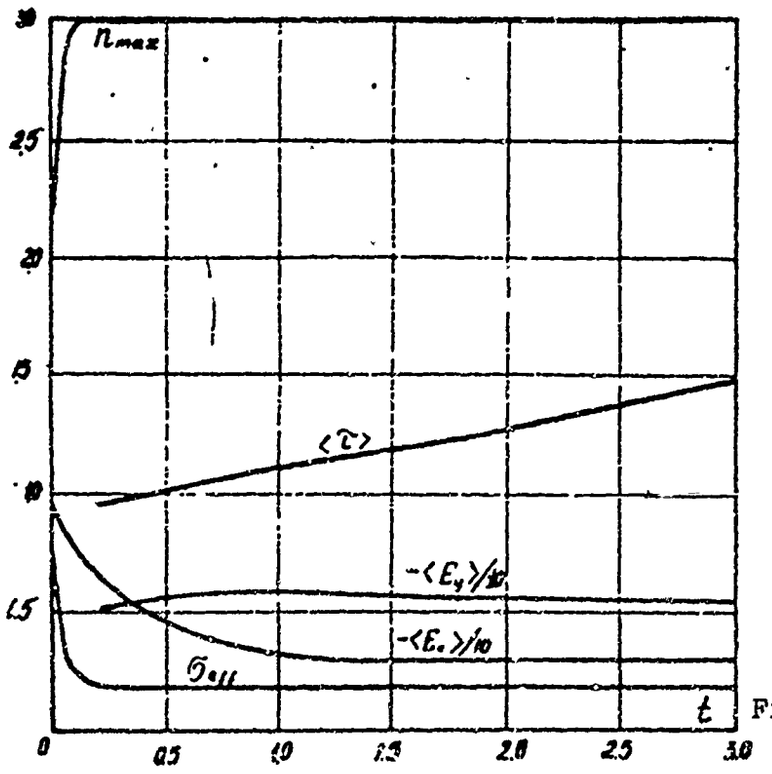

Fig. 44.

3.2. Now let us examine the same problem but in more complex geometry. We will consider that an electric current flows between the solid ideal electrodes; these comprise only a part of ab and cd of the horizontal sections of boundaries ab and cd (see Fig. 1).

An analogous problem was examined in Section 2, but with ideally sectioned electrodes; therefore henceforth the results will be compared with those of Section 2. By time t = 1 (cf. Fig. 30 and Fig. 45) which is characteristic for both problems we have a boundary layer of increased concentration of electrodes, which was discussed in Section 2. Let us note that because of the stronger concentration of current at the ends of the solid electrodes a and c and on the ends of the ideally sectioned electrodes, the formation of this layer occurs more intensely. In the center of the region at this moment with solid electrodes the current has a primarily horizontal direction, while with the ideally sectioned electrodes it was vertical. The three-dimensional distribution of current density j_x and j_y and electron concentration n_e are shown in Figs. 45-49, respectively, for times t = 1, 3, 5, 7, and 10.

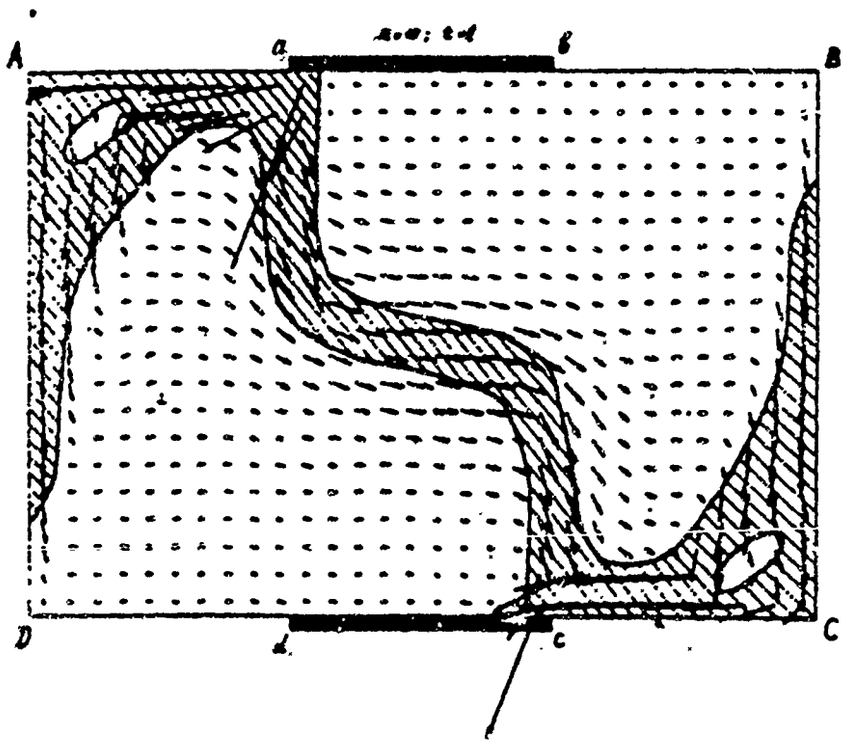

Fig. 45.

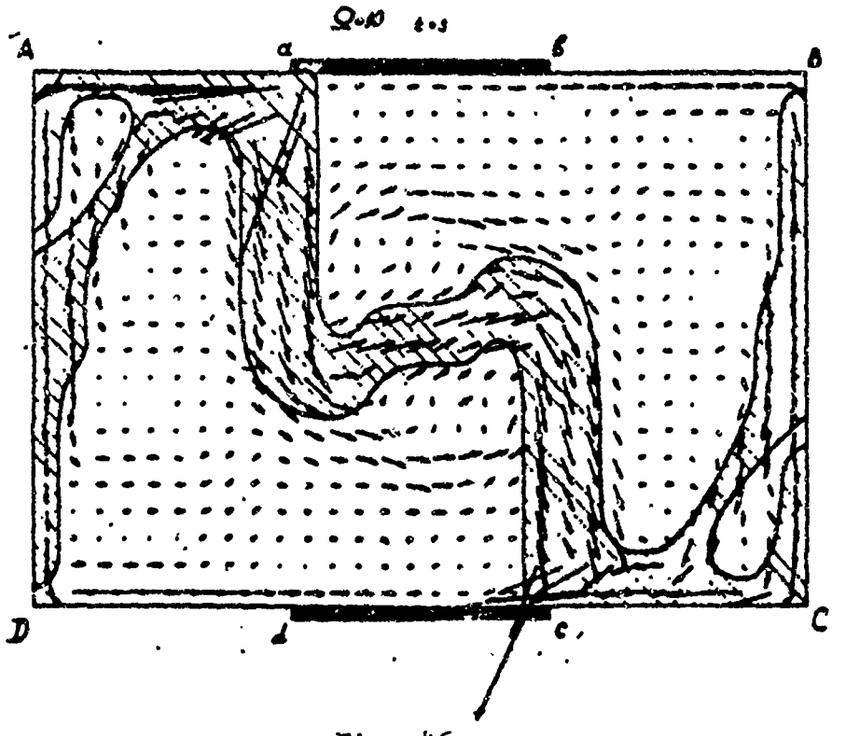

Fig. 46.

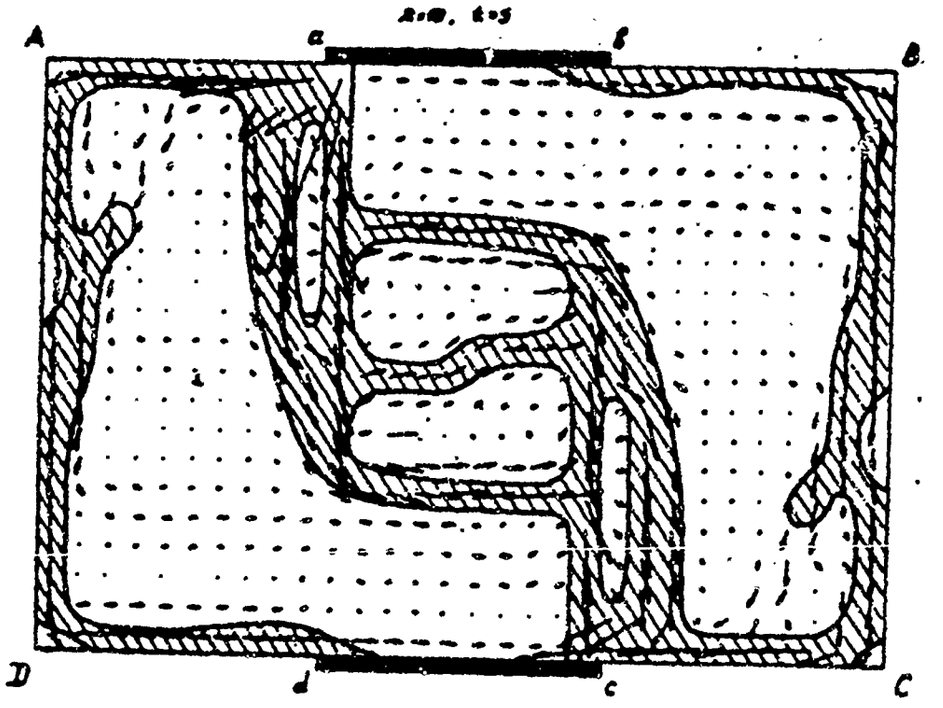

Fig. 47.

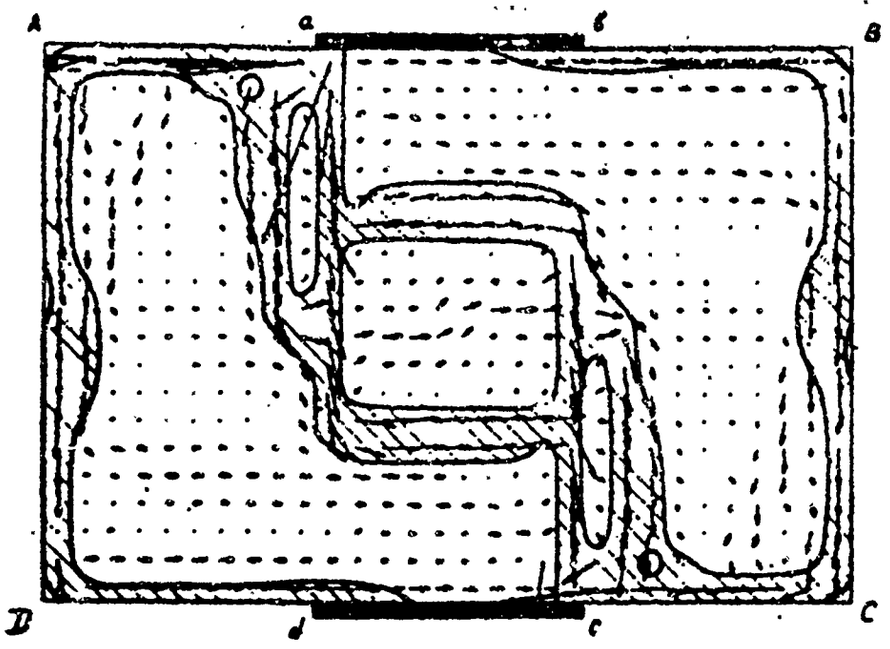

Fig. 48.

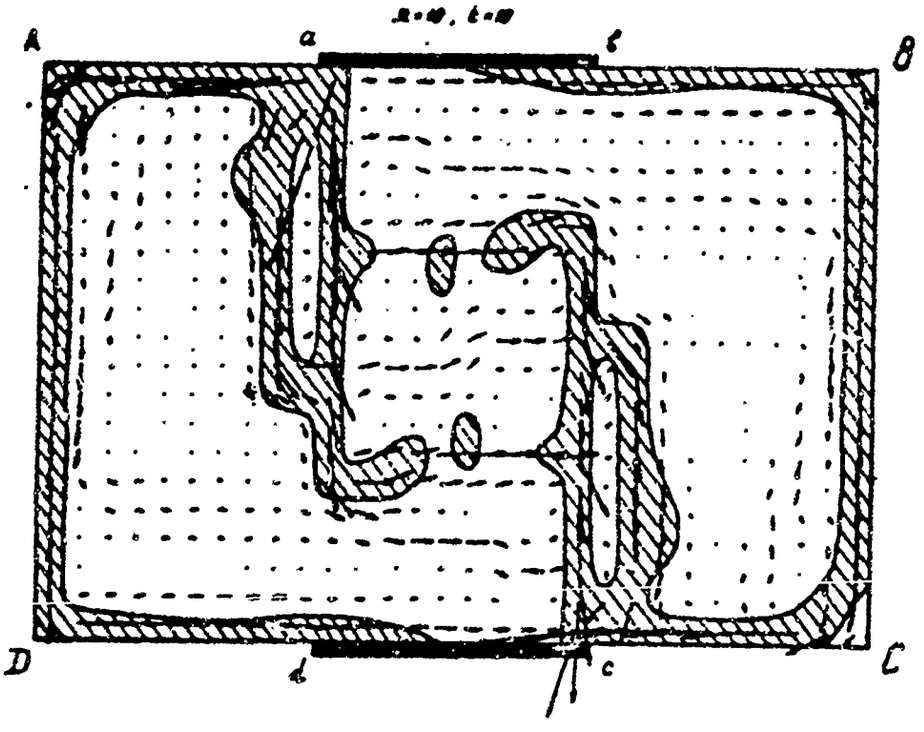

Fig. 49.

At time t = 3 the current in the center of the region, having a horizontal direction (Fig. 46), forms a striation with increased electron concentration. By time t = 5 the striation expands and disintegrates into individual horizontal "streaks."

This is explained by the fact that $E_x << E_y$ between the electrodes because of the influence of the boundary condition $E_x = 0$ on the electrodes themselves. Since the actual Hall parameter is large here (since concentration n_e is, on the average, small), the electric current flows almost perpendicular to the electric field which can effectively be identified with E_e. Thus, the electric current in the interelectrode region flows primarily parallel to the ideal electrodes. Figures 48 (t = 7) and 49 (t = 10) show further agitation of the plasma; a characteristic feature is that the current breaks down into individual streaks, having primarily horizontal direction.

Let us note that the flow of current in ideally sectioned electrodes with the same geometry and the same parameters has a different nature (see Figs. 30-34). There, by time t = 1.8, there is formed a bundle with increased electron concentration (striation) directed from the right end of the upper electrode (point b) to the left end of the lower electrode (point c). Then the plasma is agitated, but the electric current remains concentrated in the interelectrode space and breaks down into streaks which have primarily vertical direction and which are connected by bridges

Such a difference in the passage of the electric current leads to varying changes in the average values with time (cf. Fig. 35 and Fig. 50). Turbulent resistance of the plasma is approximately twice as great, while the ratio $\langle E_x \rangle / \langle E_y \rangle \simeq 0.5$ instead of the ratio $\simeq 2$ in the case of ideally sectioned electrodes.

4. Let us examine the influence of nonuniformity of the magnetic field on the passage of current between ideally sectioned electrodes in the geometry of Section 2. Let us assume that the geometry of the problem and the initial conditions at initial moment of time t = 0 are analogous to those in Section 2. The problem differs

from that in Section 2 in that the external magnetic field occurs only between electrodes; in the remaining sections of the regions it is absent. Along lines ad and bc there is an abrupt drop in the magnetic field from H ≈ 10 to H = 0. The distribution of j_x, j_y, and n_e is shown in Figs. 51, 52, and 53, for times t = 1, 5.2, and 11.6, respectively. In comparison with the corresponding problem of Section 2 (see Figs. 30-34) the picture of j_x, j_y, and n_e differs substantially. There are no layers of increased concentration along the dielectric wall (since Ω in AadD and bBCc). In these regions there is "barrel-shaped" flow of current from the upper electrode to the lower one. Discontinuity of the magnetic field along ad and bc causes discontinuity in Ω, which leads to discontinuity of the electric field intensity and the electric current density along ad and bc. With time, because of instability, there appears turbulent resistance of the plasma in the space between the electrodes; therefore the electric current flows from electrode to electrode primarily along regions AadD and bBCc (Figs. 52-53).

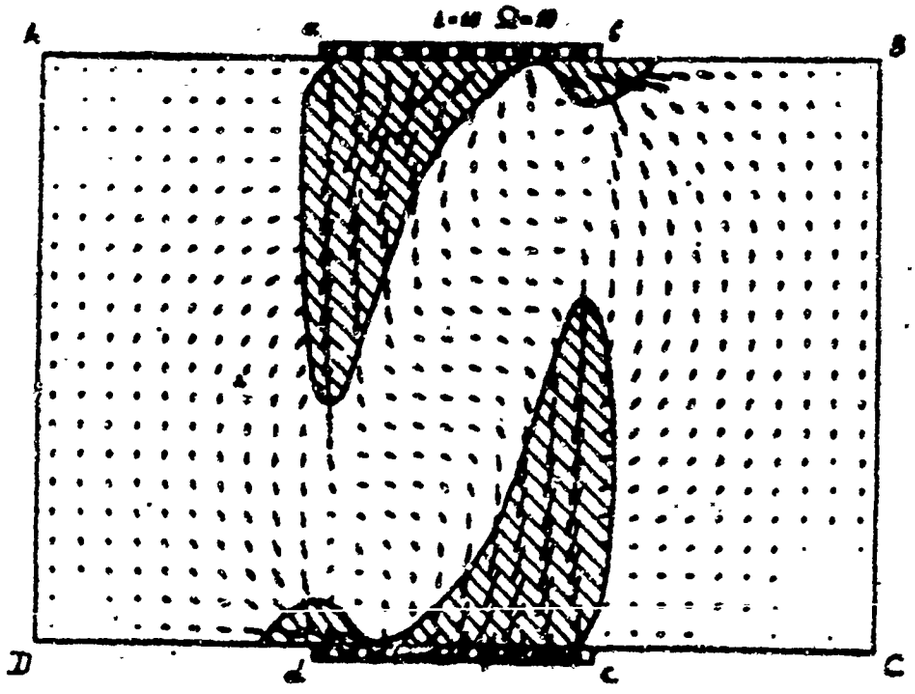

Fig. 51.

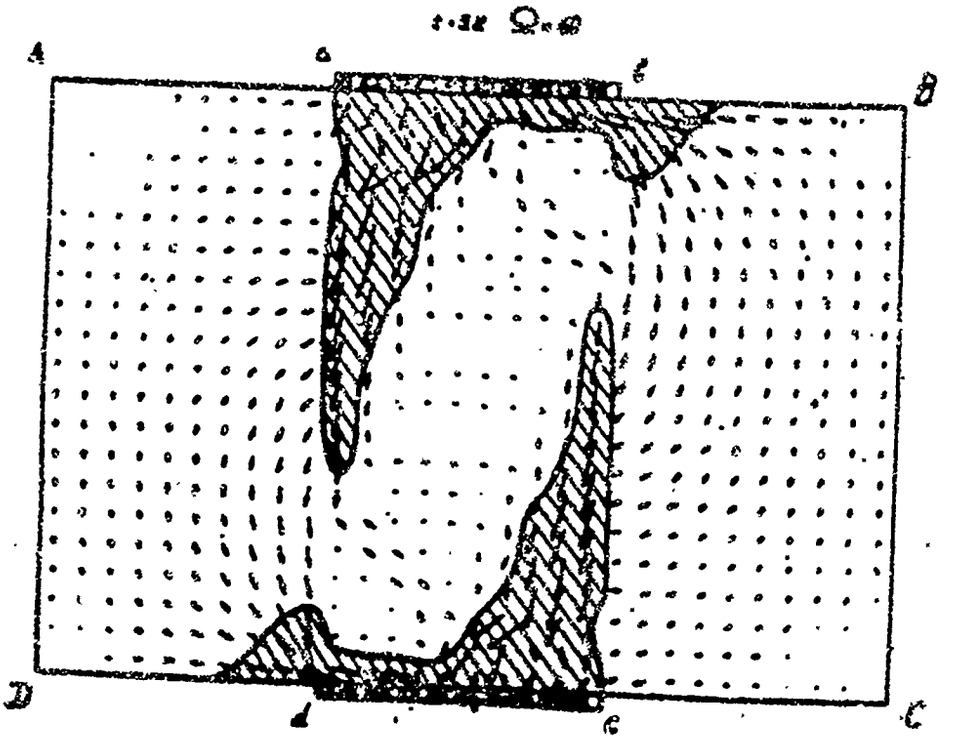

Fig. 52.

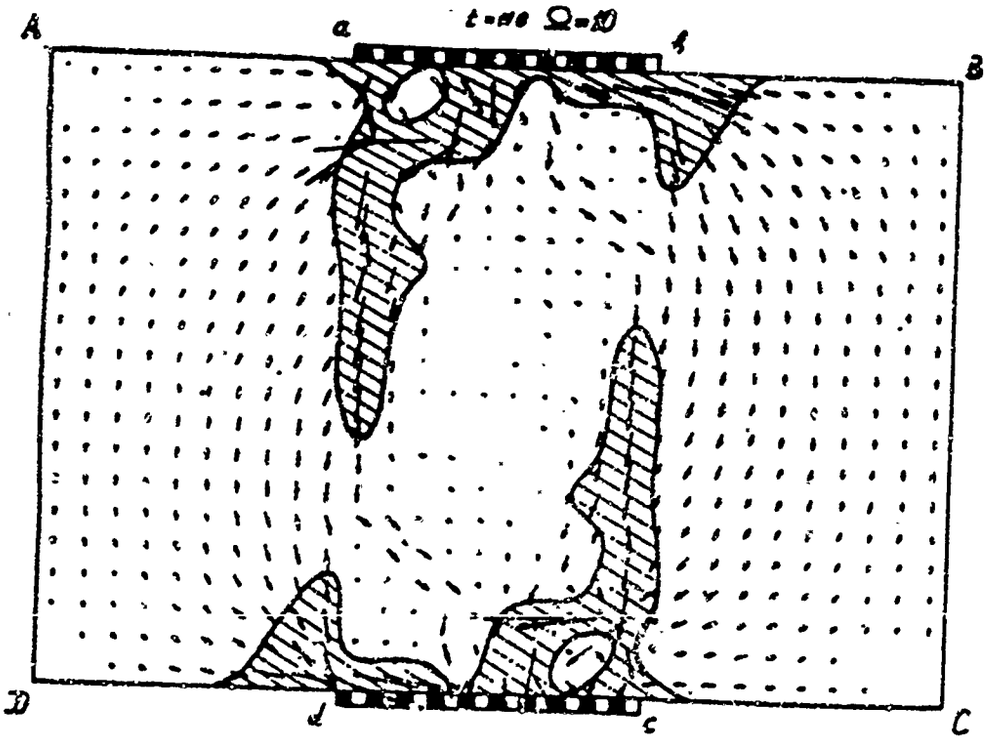

Fig. 53.

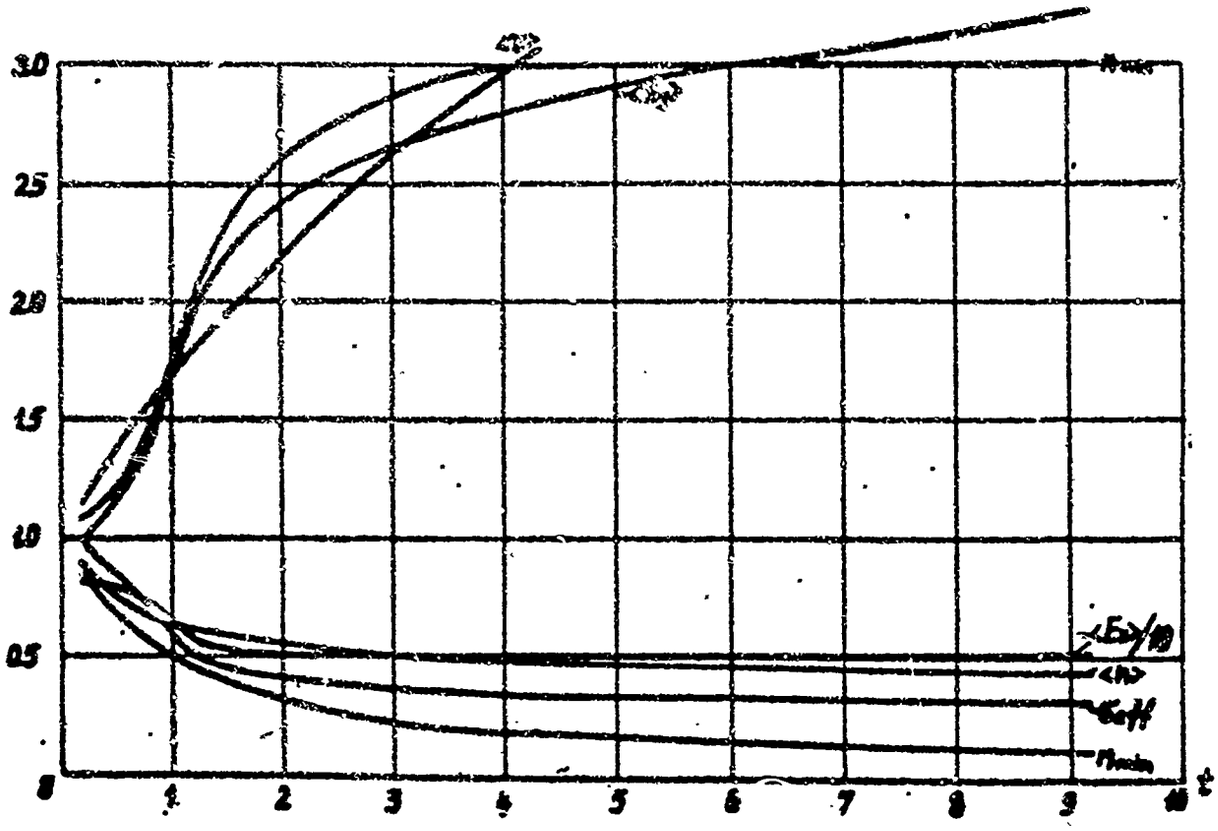

Fig. 54.

The maximum currents are concentrated near the magnetic field and electrode discontinuities, causing maximum ionization there; in the remaining space there is no current. Figure 54 shows the integral values. A comparison of them with integral values of the corresponding problem in Section 2 (Fig. 35) shows that the end effects, due to the cutoff of the magnetic field, leads to a drop (two-fold) in the Hall intensity of the electric field and an increase in turbulent resistance.

5. The problem of ionization instability in an unbounded volume, as can be seen from the initial equations, has no characteristic dimension. However, when solving it numerically, the characteristic dimension is the scale of averaging equal to the step of the difference net $\lambda = h$. When solving the problem, taking into account diffusion processes (radiation, thermal conductivity, etc.), the characteristic dimension of the problem will be the diffusion length of these processes. From this point of view, the step of the difference net can be treated as the diffusion length of certain physical processes,

while a change in step of the net corresponds to a change in certain physical parameters (mean-free path of radiation, coefficient of thermal conductivity, etc.). Let us trace the influence of the scale of averaging on the development of ionization instability. In Section 1 we examined the problem for a number of computation cells N = 200 ($h_x = h_y = 0.1$), and a perturbation was introduced into eight cells in the center of the region. Let us examine this same problem for N = 800 ($h_x = h_y = 0.05$) with a perturbation in 32 cells. A decrease in the step of the difference net leads, at time t = 1.5, to a somewhat different location of the striation (Fig. 55) than in Fig. 2. At the location of the same disturbance there occur two striations whose thicknesses, as before, are equal to several scales of averaging (several steps of the difference net). Near the boundary the striation picture is disrupted slightly, which is explained by the influence of boundary conditions. The formation of striations in this case occurs more intensely and, by moment t = 1.5, we find indications of the appearance of an irregular picture which, by moment t = 7, has little in common with the picture in Fig. 4. The development of instability at N = 800 from a perturbation occupying four cells in the center of the region is shown Figs. 56-58, corresponding to moments of time t = 1.4, 4.6, and 19.0. The local picture of j_x, j_y, and n differs from the previous problem. By time t = 1.4 (Fig. 56) there are five striations; the central striation is located at an angle close to $\pi/3$ to the total current. Then the striations are disrupted (Fig. 57) and by moment t = 19 (Fig. 58) there is strongly developed instability in the plasma. Let us note that with passage along such a plasma the current breaks down into elongated vertical streaks (5-10 characteristic dimensions) which are connected by short bridges (1-2 characteristic dimensions). Let us examine the change in time of the average values which, for N = 800, are shown in Fig. 59. Despite the varying distribution of electron concentration with time during complete perturbation in the 32nd and 8th cells the integral characteristics, beginning with moment $t^* \gtrsim 2$ coincide with good accuracy.

With a narrower step the drop in σ_{eff} and $\beta_{eff} = \langle E_x \rangle / \langle E_y \rangle$ occurs more intensely; thus, σ_{eff} decreases from 6 at N = 200 to 3.2

at N = 800. This is evidently associated with the drop in β_{eff} with decreasing step of the net.

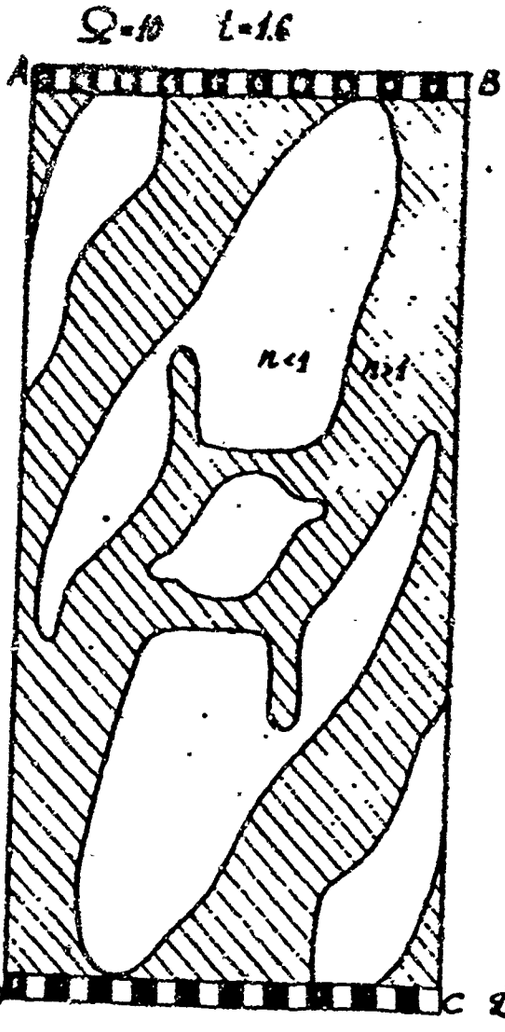

Fig. 55.

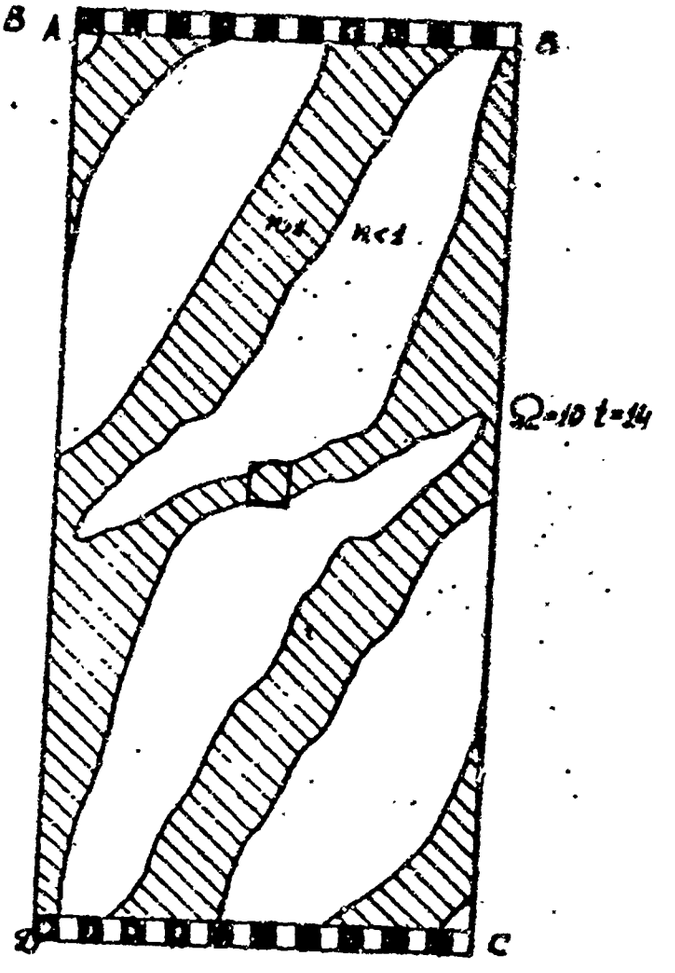

Fig. 56.

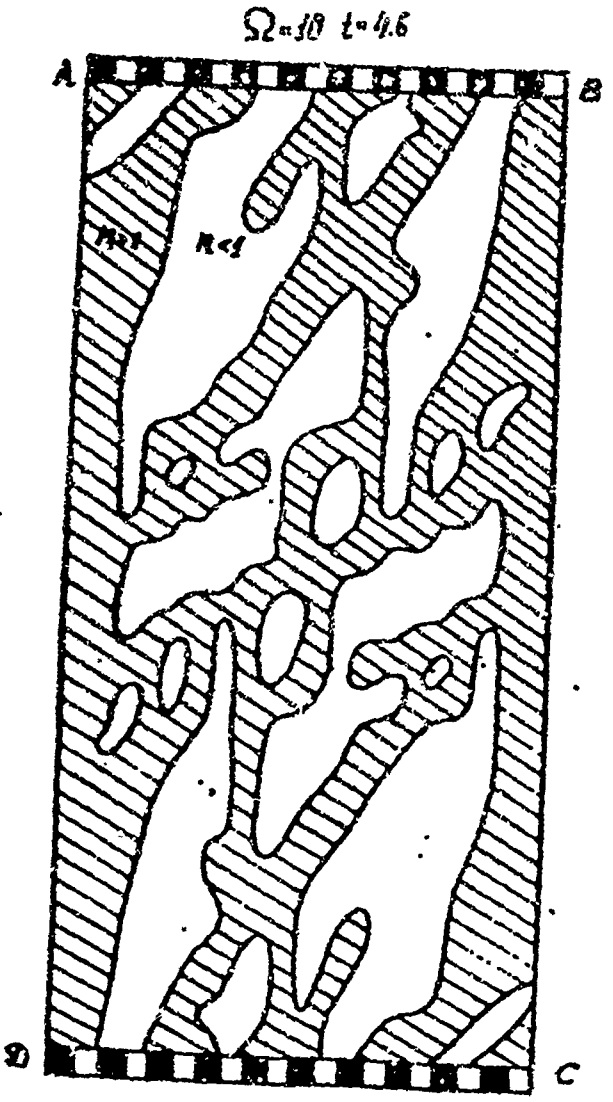

Fig. 57.

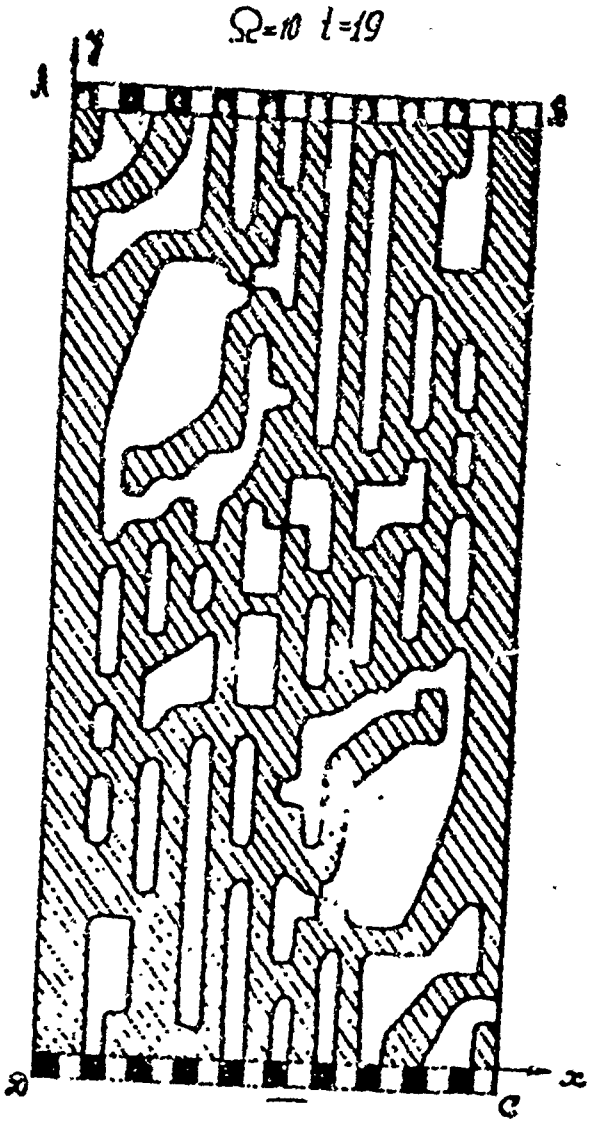

Fig. 58.

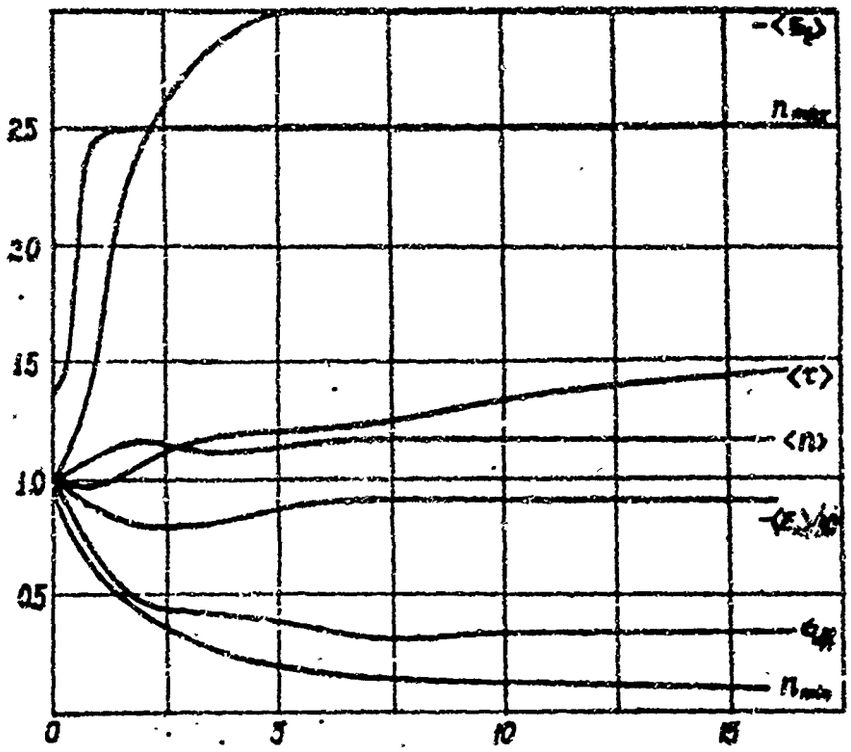

Fig. 59.

Let us illustrate the influence of a change in characteristic length of averaging λ in yet another problem. Let us assume that the ideally sectioned electrodes occupies the central region (10 intervals, h = 0.1) of the horizontal sections of the boundary along which there are 22 calculation intervals. The vertical walls occupy 20 intervals.

The geometry of this problem is the same as that of Section 2. Again we will consider the plasma to be Coulomb and, when t = 0, $j_x = 0$, $j_y = -1$ in the space between the electrodes, while $n_e = 1$ throughout the region. The distribution of j_x, j_y, and n_c at moments t = 3 and 5 is shown in Figs. 60 and 61 (only the left halves of the figures are shown). The passage of current in this problem repeats all the features noted in Section 2 (see Figs. 30-34).

The distribution of j_x, j_y, and n in this same geometry, but with h = 0.05, at moments t = 3, 5, and 7 are shown in Figs. 62-64. A comparison of Figs. 60 and 62, and also 61 and 63, shows that ionization instability develops more intensely with a shorter length

of averaging, while the turbulent stage is achieved by the plasma earlier. There is formations of current streaks having width $\sim\lambda = h$, elongated in the vertical direction ($\sim 10\lambda$), connected by short ($\sim\lambda - 2\lambda$) bridges. This can be seen in Fig. 64, which shows the distribution of j_x, j_y, and n when t = 7.

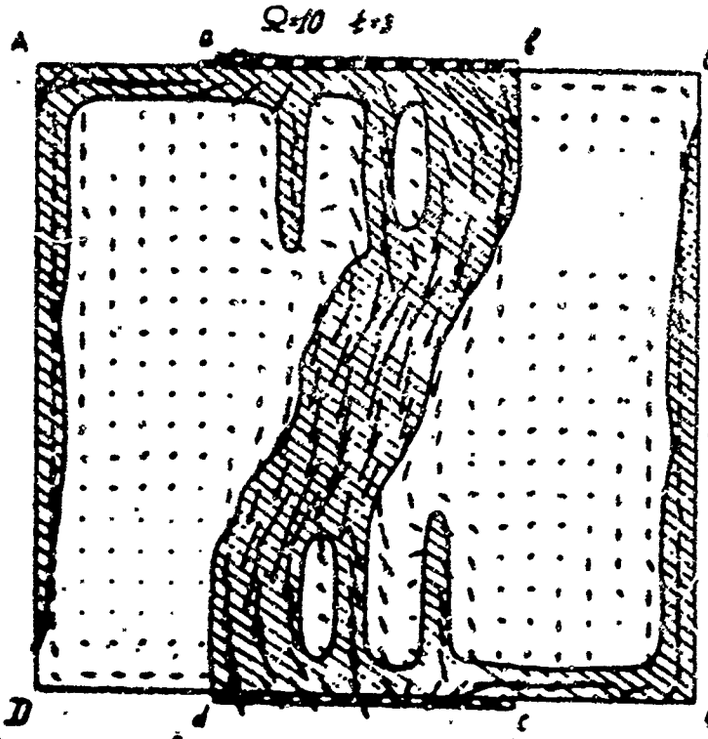

Fig. 60.

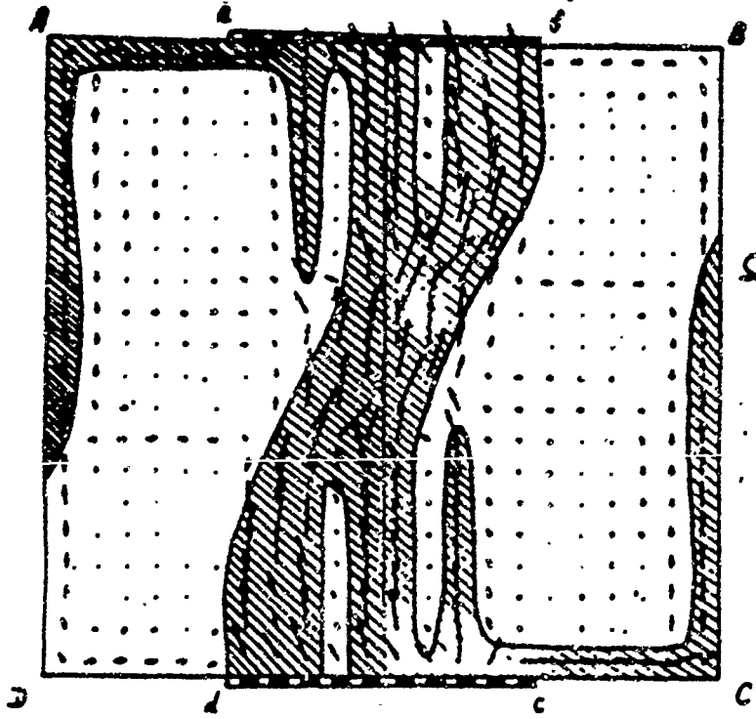

Fig. 61.

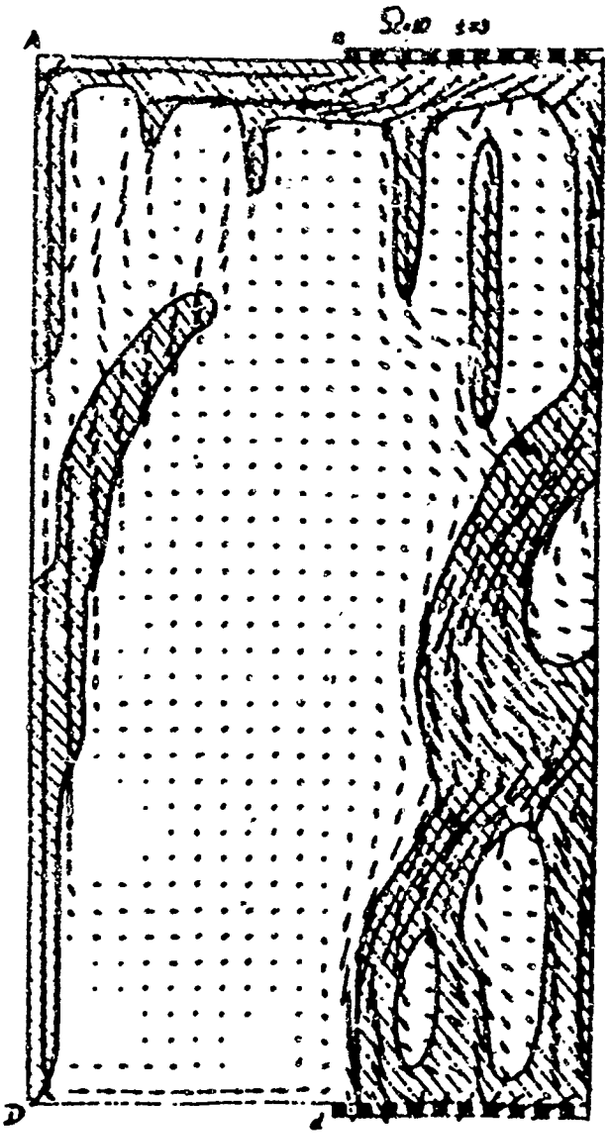

Fig. 62.

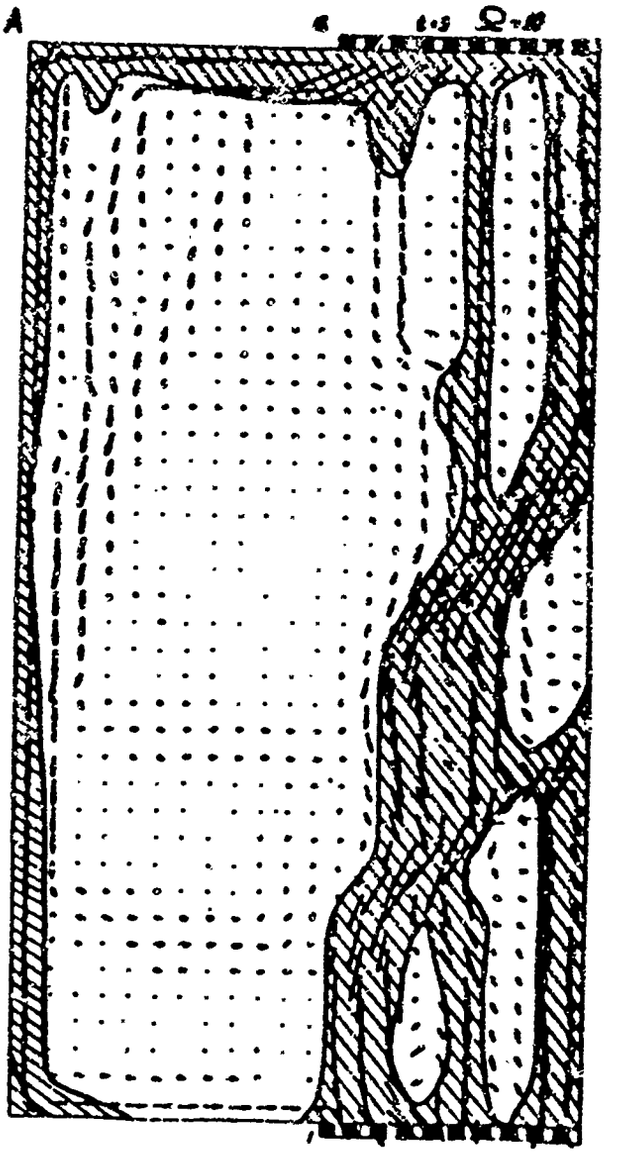

Fig. 63.

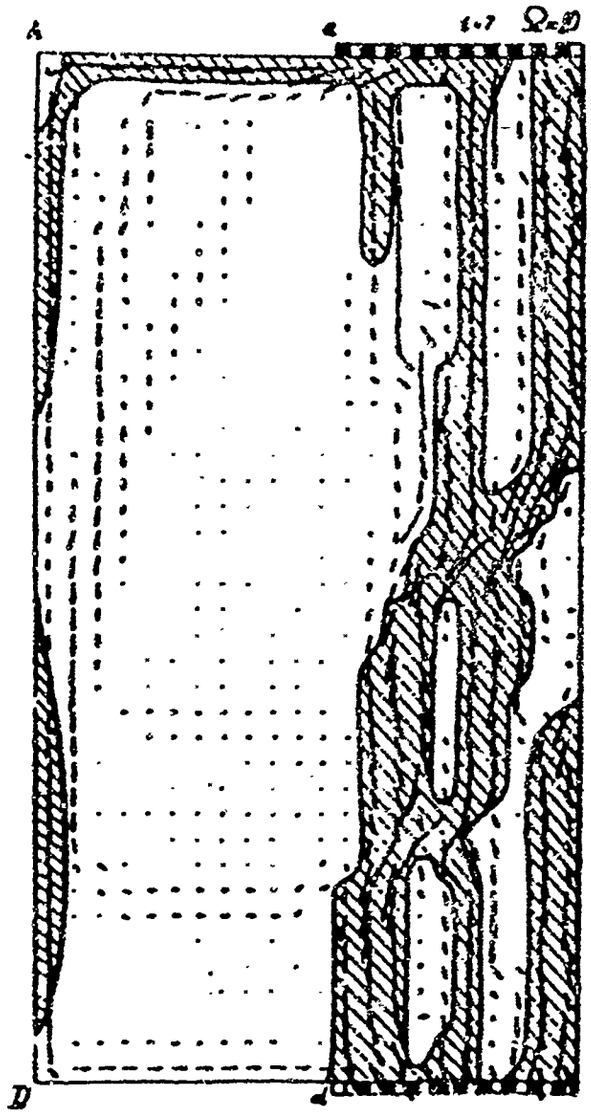

Fig. 64.

The conclusion as to the growth of turbulent resistance σ_{eff} and a drop in ratio $\langle E_x \rangle / \langle E_y \rangle$ with decreasing λ is confirmed by Fig. 65, which shows the change in integral values with time ($\lambda = h = 0.05$ – solid lines, $\lambda = h = 0.1$ – dashed lines).

$\ell \sim \langle\Omega\rangle\lambda$ the current should "leave" the streak, "breaking" it. Such "broken" streaks can cover the region only by forming "large-scale layers" (cf. [18]) of thickness $\sim\ell$. Along the continuous boundary of the large layers, electric currents pass in turn. As numerical calculations show, here there are formed current bundles with increased concentration n_e, which can be identified with striations. The striations have a thickness of the order of several scales of averaging and are elongated (parallel to each other) at a certain angle to the average current (see Fig. 58). The value of the angle corresponds, apparently, with the direction of most intense release of Joule heat. This corresponds with the fact that electron concentration and current density in the striations are considerably higher than in the streaks. In the calculations we observed the angle $\sim\frac{\pi}{4} - \frac{\pi}{3}$. The value $\pi/4$ corresponds to the solution of the problem on the development of one-dimensional perturbations.

7. Let us present the results of characteristic calculations with $H \gg 1$, described above, in the form of Table 1 (Fig. 66). Let us explain the designations. The region occupied by the plasma is arbitrarily divided into two types: The first type includes a region whose horizontal sections are entirely covered by the electrodes; the second type includes the region whose horizontal sections contain dielectric portions. The other designations are clear from what has been said above. The values of the effective parameters, presented in the table, satisfy the following relationship quite accurately:

The values of the effective parameters, presented in the table, satisfy the following relationship quite accurately:

$$\sigma_{eff} = \sigma_0 \frac{\beta_{eff}}{\Omega_0} \tag{5.1}$$

where Ω_0 and σ_0 are values corresponding to uniform distribution of the plasma parameters, i.e., $\sigma_0 = 1$, $\Omega = \frac{H}{n_0} = H$. Let us turn our attention to the fact that relationship (5.1) is invariant with respect to type of electrode and region, scale of averaging λ, and also ratio A_2/A_1, which characterizes the presence of a neutral component. The validity of (5.1) is also confirmed by the results of all other numerical calculations. An exception is that line of the table,

indicated by an asterisk, which corresponds to the case when the magnetic field occurs only in interelectrode space. Let us remember, however, that the electric current in this case flows almost completely from the interelectrode region and occurs laminarly along a non-magnetized plasma, while (5.1) obtains for a plasma with a strongly developed instability.

Table 1.

Points	Dimension of averaging	Type of region	Type of electrode	β_{eff}	σ_{eff}	Ω_0	<n>	<β>	Remarks
1.	0.1	1	ideally sectioned	3.5	0.4	10	1.05	11.2	a neutral component exists
2.	0.1	1	ideally sectioned	5.5	0.55	10	–	17	
3.	0.1	1	solid	2	0.2	10	–	14.8	
4.	0.05	1	ideally sectioned	2.5	0.32	10	1.2	14.4	
5.	0.1	2	solid	0.6	0.06	10	–	–	
6.	0.05	2	ideally sectioned	2	0.2	10	–	–	
7.	0.1	1	ideally sectioned	3.6	0.75	5	–	–	
*8.	0.1	2	ideally sectioned	1.6	0.3	10	–	–	magnetic field between the electrodes

Relationship (5.1) can be obtained approximately as follows. Analogous to [18], let us examine a layer of plasma between striations, developed along the streaks. Let us direct axis x perpendicular to the streaks and axis y along them (parallel to the average current). Setting $\langle\Omega\rangle \gg 1$ we can consider that $j_x \ll \Omega_{jy}$. Actually, in the streaks, $j_y \gg j_x$ (obviously), while between them, $\Omega \gg 1$. Thus in the equation

$$j_x + \Omega_{jy} - \sigma E_x$$

the component j_x can be discarded, i.e.,

$$j_x = \frac{\sigma}{\Omega} E_x = \frac{n_e E_x}{H}.$$

Let us average this equality, without considering the correlation between n_e and E_x:

$$\langle j_y \rangle = \frac{\langle n_e E_x \rangle}{H} \simeq \frac{\langle n_e \rangle \langle E_x \rangle}{H}.$$

From this,

$$\sigma_{eff} = \frac{\langle j_x \rangle}{\langle E_y \rangle} = \frac{\langle n_e \rangle}{H} \frac{\langle E_x \rangle}{\langle E_y \rangle} = \frac{n_e}{H} \beta_{eff}.$$

Since in numerical calculations $\langle n_e \rangle \simeq 1$, we can write, finally, setting $n_0 = \sigma_0 = 1$,

$$\sigma_{eff} = \sigma_0 \frac{\beta_{eff}}{\Omega_0}.$$

In the derivations we did not consider currents in striations on the boundaries of the layers. But since the thickness of each stratum is smaller than the thickness of the layer by a factor of Ω_0, while the current in it is limited, then when $\Omega_0 \gg 1$ the "contribution" of striations to the average parameters of the plasma can be disregarded. Finally, if we assume that when $\lambda \ll 1$ the equality $\beta_{eff} = \beta_{cr}$ is nonetheless valid, we get

$$\sigma_{eff} = \frac{\sigma_0}{\Omega_0} \beta_{cr}.$$

We should, however, stress that such an approach must be founded.

CHAPTER 6

CONCLUSIONS

On the basis of an analysis of the results of numerical solution of the problem of the development of ionization instability in a magnetized plasma we can draw the following conclusions.

1. The physical model used qualitatively reflects the essence of the phenomenon and the characteristic moment known from the experiment:

a. The nonlinear mechanism of Joule heating and transfer of energy during collisions of electrons with a heavy component causes, in characteristic time t^*, the appearance of ionization instability as regular formations — striations.

b. In later stages of the process ($t >> t^*$) there is decay of the primary striations, leading to irregular three-dimensional distribution of electron concentration and electric current density. Nonetheless, when $t >> t^*$ we speak of the structure of an irregular picture, which consists of the following. An electric current passes mainly in the "streaks" parallel to the direction of the average current. The thickness of the streaks and the difference between them $\sim\lambda$, while their length $\sim\langle\Omega\rangle\lambda$, where λ is the characteristic scale of averaging. Between the streaks the current density and concentration n_e are relatively low. The streaks are joined into layers along whose continuous boundaries there are strong electrical

currents, forming striations with high electron concentration. The angle between striation and the direction of the average current $\sim\frac{\pi}{4} - \frac{\pi}{3}$; the thickness of the striations is of the order of several scales of averaging.

c. On the electrodes and the dielectric regions adjacent to them there are layers with increased electron concentration; these were observed by Kerrebrock.

d. The presence of a nonmagnetized region of plasma leads to emergence of the electrical field into this region.

2. Despite the locally nonstationary picture of developed instability there occurs an establishment of average and effective parameters of the plasma in certain characteristic times t^*. Here we should note the following:

a. The steady-state average and effective parameters of the plasma, generally speaking, depend on the type of electrode, the geometry of the region, the presence of a neutral component, and the scale of averaging λ, and do not depend on the initial condition.

b. The effective parameters of the plasma are connected by the relationship

$$\sigma_{eff} = \frac{\sigma_0}{\Omega_0}\beta_{eff}$$

which is invariant with respect to the geometry of the region, the type of electrode, the presence of a neutral component, and the scale of averaging λ.

3. We have refined the statistical picture of strongly developed instability:

a. There is angular anisotropy in the distribution of the electron concentration relative to the direction of the average current, which is released.

b. There is, generally speaking, no mirror symmetry of distribution of electron concentration with area.

4. The boundary conditions have a substantial influence on the process of development of instability and the final state of the plasma:

a. Between the ideally-sectioned electrodes the current passes primarily in a direction orthogonal to the plane of electrodes.

b. Between the solid ideal electrodes the current in the interelectrode region is directed primarily parallel to the electrode plane.

c. The average and effective parameters of the plasma, with $t >> t^*$, as already noted, depend on the boundary conditions.

5. A decrease in the characteristic scale of averaging leads to a reduction in the first stage of the process (time t^* of the formation of striations and decrease of β_{eff} (however β_{eff} is always greater than β_{cr})).

6. Consideration of collisions of electrons with a neutral component does not change substantially the qualitative nature of the development of instability and the final state of the plasma.

The authors would like to thank A. A. Samarskiy for his valuable discussions and Ye. Ye. Myshetskaya for compiling the programs and carrying out the calculations.

References

1. Velikhov, Ye. P. Doklad na I Mezhdunarodnom simpoziume po MGD preobrazovaniyu energii. N'yukasl (Report at 1st International Symposium on the MHD Conversion of Energy. Newcastle), 1962.

2. Velikhov, Ye. P., and A. M. Dykhne. Comptes rendus de la IV Conference international sur les phenomenes d'ionisation dans les gas, Paris, Vol. 2, 1963, p. 511.

3. Kerrebrock, J. L. AIAA, 2, 1072, 1964.

4. Nedospasov, A. V., and I. Ya. Shipuk. Teplofizika vysokikh temperatur 3, 186 (1965).

5. Velikhov, Ye. P., A. M. Dykhne, and I. Ya. Shipuk. Doklad na VII Mekhdunarodnoy konferentsii po ionizats. yavleniyam m gazakh. Belgrad (Report at 7th International Conference on Ionization Phenomena in Gases. Belgrade), 1965.

6. Belousov, V. N., V. V. Yeliseyev, and I. Ya. Shiduk. Proceedings of a Symposium of MHD, Salzburg, Vol. 2, p. 355, 1966.

7. Kleipies, J. K., and R. J. Rosa. AIAA, 3, 1659, 1965.

8. Vitmas, A. F., V. S. Golubev, and M. M. Malikov. Proceedings of a Symposium of MHD, Salzburg, Vol. 2, 1966.

9. Vitmas, A. F., V. S. Golubev, and M. M. Malikov. Proceedings of a Symposium of MHD, Warsaw, 1968.

10. Louis, J. F. 8th Symposium of Engineering Aspects of MHD, Stanford, 1967.

11. Kleipies, J. 10th Symposium of MHD, Boston, 1969.

12. Brederlow, W. Feneberg, and G. Hadson. Proceedings of a Symposium of MHD, Salzburg, Vol. 2, p. 29, 1966.

13. Brederlow, W. Feneberg, and G. Hadson. Proceedings of a Symposium of MHD, Warsaw, 1968.

14. Dethlesson, R., and J. K. Kerrebrock. 7th Symposium on Engineering Aspects of MHD, Princton, 1966.

15. Solbes, A. 8th Symposium on Engineering Aspects of MHD, Stanford, 1967.

16. Milora, S. L. Nonlinear Plane Wave Studies of Electrothermal Instabilities, Transactions of Pennsylvania State University, 1967.

17. Vedenov, A. A., and Ye. P. Velikhov. Proceedings of a Symposium of MHD, Salzburg, Vol. 2, 1966.

18. Vedenov, A. A., and A. M. Dykhne. Proceedings of a Symposium of MHD, Salzburg, Vol. 2, 1966.

19. Dykhne, A. M. Proceedings of a Symposium of MHD, Warsaw, 1968.

20. Solbes, A. Proceedings of a Symposium of MHD, Warsaw, 1968.

21. Zampalioni. Proceedings of a Symposium of MHD, Warsaw, 1968.

22. Gurashvili, Kareyev, and A. V. Nedospasov. Preprint IAE, 1968.

23. Velihhov, Ye. P., L. M. Degtyarev, A. A. Samarskiy, and A. P. Favorskiy. Shestoye rizhskoye soveshchaniye po magnitnoy gidrodinamike (Sixth Riga Conference on Magnetohydrodynamics).

24. Velikhov, Ye. P., L. M. Degtyarev, A. A. Samarskiy, and A. P. Favorskiy. DAN, Vol. 184, No. 3.

25. Velikhov, Ye. P., L. M. Degtyarev, A. A. Samarskiy, and A. P. Favorskiy. 10th Symposium on Engineering Aspects of MHD, Boston, 1969.

26. Lenguel, L. L. 10th Symposium on Engineering Aspects of MHD, Boston, 1969.

27. Tikhonov, A. N., and A. A. Samarskiy. Zh. vychisl. matem. i matem. fiz. I, 1961, No. 1.

28. Samarskiy, A. A. Zh. vychisl. matem. i matem. fiz. 4, 1964, No. 5.

29. Degtyarev, L. M., A. A. Samarskiy, and A. P. Favorskiy. Chislennoye resheniye vnutrennikh statsionarnykh zadach elektrodinamiki (Numerical solution of internal stationary problems of electrodynamics).

30. Zel'dovich, Ya. B., and Yu. P. Rayzer. Fizika udarnykh voln i vysokotemperaturnykh gidrodinamicheskikh yavleniy (The physics of shock waves and high-temperature hydrodynamic phenomena), Moscow, 1966.

31. Spitzer, L. Physics of fully ionized gases. New York, Interscience Publishers, 1962. 170 pp. [Russian translation, same title, published Moscow, Izd. "Mir," 1965].

32. Sutton, G. W., and A. Sherman. Engineering magnetohydrodynamics. New York, McGraw-Hill Book Co., 1965. 548 pp. [Russian translation, same title].

UNCLASSIFIED
Security Classification

DOCUMENT CONTROL DATA - R & D

(Security classification of title, body of abstract and indexing annotation must be entered when the overall report is classified)

1. ORIGINATING ACTIVITY (Corporate author)	2a. REPORT SECURITY CLASSIFICATION
Foreign Technology Division Air Force Systems Command U. S. Air Force	UNCLASSIFIED
	2b. GROUP

3. REPORT TITLE

NUMERICAL STUDY OF IONIZATION INSTABILITY IN LOW-TEMPERATURE MAGNETIZED PLASMA

4. DESCRIPTIVE NOTES (Type of report and inclusive dates)

Translation

5. AUTHOR(S) (First name, middle initial, last name)

Velikhov, Ye. P., Degtyarev, L. M. and Favorskiy, A. P.

6. REPORT DATE	7a. TOTAL NO. OF PAGES	7b. NO. OF REFS
1969	76	32

8a. CONTRACT OR GRANT NO.	9a. ORIGINATOR'S REPORT NUMBER(S)
b. PROJECT NO. 72301-78	FTD-HT-23-241-70
c.	9b. OTHER REPORT NO(S) (Any other numbers that may be assigned this report)
d.	

10. DISTRIBUTION STATEMENT

Distribution of this document is unlimited. It may be released to the Clearinghouse, Department of Commerce, for sale to the general public.

11. SUPPLEMENTARY NOTES	12. SPONSORING MILITARY ACTIVITY
	Foreign Technology Division Wright-Patterson AFB, Ohio

13. ABSTRACT

In this work we examine the statement and numerical solution of the problem of the development of ionization instability in a low-temperature magnetized plasma. Basic attention is devoted to the dynamics of the development of instability and a qualitative analysis of the phenomenon. We show the effectiveness of the physical model used as the basis of the examination. As a result of the numerical calculations we refine the association between the average parameters of the plasma at process stages close to turbulence.

DD FORM 1 NOV 65 1473

UNCLASSIFIED
Security Classification

14. KEY WORDS	LINK A		LINK B		LINK C	
	ROLE	WT	ROLE	WT	ROLE	WT
Low Temperature Plasma Plasma Instability Ionization Numeric Solution Plasma Magnetic Field						